

# *How well are Tropical Cyclones represented in reanalysis data sets?*

Article

Accepted Version

Hodges, K. ORCID: <https://orcid.org/0000-0003-0894-229X>, Cobb, A. and Vidale, P. L. ORCID: <https://orcid.org/0000-0002-1800-8460> (2017) How well are Tropical Cyclones represented in reanalysis data sets? *Journal of Climate*, 30 (14). pp. 5243-5264. ISSN 1520-0442 doi: <https://doi.org/10.1175/JCLI-D-16-0557.1> Available at <https://centaur.reading.ac.uk/70250/>

It is advisable to refer to the publisher's version if you intend to cite from the work. See [Guidance on citing](#).

To link to this article DOI: <http://dx.doi.org/10.1175/JCLI-D-16-0557.1>

Publisher: American Meteorological Society

All outputs in CentAUR are protected by Intellectual Property Rights law, including copyright law. Copyright and IPR is retained by the creators or other copyright holders. Terms and conditions for use of this material are defined in the [End User Agreement](#).

[www.reading.ac.uk/centaur](http://www.reading.ac.uk/centaur)

**CentAUR**

Central Archive at the University of Reading

Reading's research outputs online



1 **How Well are Tropical Cyclones Represented in Reanalysis Data Sets?**

2 Kevin Hodges\*

3 *Department of Meteorology, University of Reading, Reading, United Kingdom*

4 Alison Cobb

5 *Department of Meteorology, University of Reading, Reading, United Kingdom*

6 Pier Luigi Vidale

7 *National Centre for Atmospheric Science, Department of Meteorology, University of Reading,*  
8 *Reading, United Kingdom*

9 *\*Corresponding author address: Department of Meteorology, University of Reading, Reading,*

10 *United Kingdom.*

11 **E-mail: [k.i.hodges@reading.ac.uk](mailto:k.i.hodges@reading.ac.uk)**

## ABSTRACT

12 Tropical cyclones (TCs) are identified and tracked in six recent reanalysis  
13 data sets and compared with those from the IBTrACS best track archive. Re-  
14 sults indicate that nearly every cyclone present in IBTrACS over the period  
15 1979-2012 can be found in all six reanalyses using a tracking and matching  
16 approach. However, TC intensities are significantly under-represented in the  
17 reanalyses compared to the observations. Applying a typical objective TC  
18 identification scheme, it is found that the largest uncertainties in TC identi-  
19 fication occur for the weaker storms; this is exacerbated by uncertainties in  
20 the observations for weak storms and lack of consistency in operational pro-  
21 cedures. For example, it is unclear whether certain types of storms, such as  
22 tropical depressions, subtropical cyclones and monsoon depressions, are in-  
23 cluded in the best track data for all reporting agencies. There are definite im-  
24 provements in how well TCs are represented in more recent, higher resolution  
25 reanalyses; in particular MERRA2 is comparable with the NCEP-CFSR and  
26 JRA55 reanalyses, which perform significantly better than the older MERRA  
27 reanalysis.

## 28 **1. Introduction**

29 Tropical cyclones (TCs) are one of the most damaging weather-related natural hazards on the  
30 planet, causing 42 % of the United States catastrophe-insured losses in the period 1992-2011  
31 (King 2013). Individual intense events can result in severe losses. For example, Hurricane Katrina  
32 resulted in an estimated death toll of 1,833 people and financial losses of over \$125 billion (Adeola  
33 and Picou 2014). Weaker storms, such as tropical depressions can also have an impact in terms of  
34 loss of life and disruption in vulnerable societies (for the Caribbean 2009). It is therefore important  
35 to utilise the available data and new analysis techniques to better understand their properties and  
36 behaviour, with the aim of mitigating their societal, economic and environmental impacts.

37 Due to the relatively short observational record of TCs, and problems with sampling within  
38 the record, there is considerable uncertainty in the variability of TCs in terms of frequency, over  
39 climate time scales of the last 100 years (Landsea 2007; Landsea et al. 2009), resulting in un-  
40 certainty in the interannual variability and trend detection. The use of reanalyses to detect TCs  
41 provides an opportunity to reduce this uncertainty (Truchelut et al. 2013), by allowing the creation  
42 of a larger data sample which, when used in conjunction with the historic observational data, can  
43 help to provide more confidence in TC numbers than the observations alone. Reanalyses combine  
44 observations with a short forecast from a general circulation model (GCM) to produce gridded  
45 data sets with regular output intervals constrained by the observations, and can act as a bridge  
46 between the observations of TCs and simulated tempestology. However, there can be problems in  
47 using reanalyses related to the changing observing system, in particular the introduction of spuri-  
48 ous trends (Bengtsson et al. 2004a), and the fact that different reanalyses use different GCMs with  
49 different parameterizations and different data assimilation methods, all of which can contribute  
50 to differences between them. The study of Schenkel and Hart (2012) previously considered the

51 representation of TCs in the northern hemisphere in several reanalyses, including several of those  
52 used in this study, by manually tracking the best track TCs in the reanalyses, and found consid-  
53 erable variation in the properties of TCs between the reanalyses, for location, and a consistently  
54 large underestimate of intensity (10m winds and Mean Sea Level Pressure) for all the reanalyses.  
55 This uncertainty in the representation of TC properties in reanalyses can introduce uncertainty into  
56 their detection in these data, so that detection criteria are often tailored to the particular reanalysis  
57 of interest (Murakami 2014).

58 Another motivation for a careful study of the properties of TCs as represented by reanalyses  
59 is that they are often used as a means of calibrating TC detection and tracking schemes before  
60 applying them to climate models (Bengtsson et al. 2007a). This is done by first applying the  
61 detection to the reanalyses or operational analyses and adjusting the detection criteria to give  
62 similar numbers of TCs to those found in the observations, provided by the TC warning centers  
63 best track data. This may be problematic if there are large differences between how reanalyses  
64 represent TCs in terms of their properties, such as structure and intensities, or if there are biases  
65 in the best track data. The model dynamical core, parameterizations and resolution all play a  
66 critical role in determining the output of extreme events in reanalysis data. These vary widely,  
67 with in particular newer generations of reanalyses being produced at higher resolutions and with  
68 more modern data assimilation systems. For climate models, the IPCC 5th Assessment (2013)  
69 stated that there is medium evidence and high agreement that year-to-year count variability of  
70 Atlantic hurricanes can be well simulated by modest resolution (100 km or finer) atmospheric  
71 GCMs (AGCMs) forced by observed Sea Surface Temperatures (SSTs). Both Strachan et al.  
72 (2013) and Roberts et al. (2015) show that 60 km is adequate for simulating interannual variability,  
73 although not intensity. Recent work by Murakami (2014) showed that, when considering five  
74 reanalyses (also included in this study), the highest resolution reanalysis was not always the best

75 in terms of simulating the TC climatology and properties, nor did the higher-resolution reanalyses  
76 produce significantly more intense storms than those with lower resolutions, suggesting that the  
77 simulation of TCs in the reanalyses is highly dependent on model formulation (Schenkel and Hart  
78 2012) and/or data assimilation strategy. However, if we can understand the uncertainties of TCs  
79 in the reanalyses, they may provide a useful means of extending the observations, for example,  
80 by extending their lifecycles to include the extratropical transition (Jones et al. 2003) and beyond,  
81 which would be useful for TC related extratropical risk analysis and GCM assessment (Haarsma  
82 et al. 2013). The use of reanalysis could also assist in the identification of subtropical and hybrid  
83 tropical storms (Roth 2002; Guishard et al. 2009), which are also associated with severe weather,  
84 providing a more complete set of tropical storm data for use in GCM assessment than is perhaps  
85 currently present in best track data; the inclusion of these types of storms in the best track data sets  
86 is highly variable between the operational centres.

87 The main aim of this paper is to quantify the uncertainties in how well TCs are represented in a  
88 number of recent reanalyses, and how this affects the objective identification of TCs in reanalyses.  
89 This is achieved by exploring:-

- 90 1. how well reanalyses represent the observed TCs in the best track data using direct track  
91 matching.
- 92 2. how well does an objective identification scheme identify the best track TCs in the reanalyses  
93 and what might be the cause of differences.

## 94 **2. Data and Methods**

95 Data from six recent reanalyses are used in this study and described below. Also used are best  
96 track data produced by the tropical warning centers as post season analyses of the TC tracks. These

97 have been combined into the International Best Track Archive for Climate Stewardship (IBTrACS)  
98 data set (Knapp et al. (2010)) and are used in this study for verifying the TCs identified in the  
99 reanalyses. The IBTrACS-ALL, which includes data from all agencies, is used in this study. The  
100 common period of 1979-2012 is used throughout for all data sets, except for one reanalysis where  
101 the period is 1980-2012. Throughout the rest of the paper the following nomenclature is used; the  
102 term Tropical Cyclone (TC) is used for warm core storms generally and, where appropriate, the  
103 term Tropical Storm (TS) is used for TCs with wind speeds greater than  $17 \text{ m s}^{-1}$ .

#### 104 *a. Best Track dataset*

105 For full details of the IBTrACS-ALL data set, see Knapp et al (2012). The original wind speed  
106 data in knots is converted to wind speed in  $\text{m s}^{-1}$ . The World Meteorological Organization (WMO)  
107 standard for reported tropical cyclone wind speed is maximum 10-minute sustained winds at 10  
108 m height over a smooth surface; however, this is rarely observed, therefore some discrepancy be-  
109 tween agencies is apparent. Different agencies apply different wind-averaging periods, with the  
110 East Pacific, North Atlantic (RSMC Miami), and central Pacific (RSMC Honolulu) using 1-minute  
111 averaging periods, North Indian (RSMC New Delhi) using a 3-minute period and the other agen-  
112 cies using 10-minute averaging periods (Schreck III et al. 2014). The 10-minute wind speeds  
113 are converted to 1-minute wind speeds using a factor of 1.13, which has traditionally been used  
114 (Harper et al. 2010), and the data from RSMC Miami and New Delhi are used in their original  
115 form. However, there are uncertainties in the accuracy and fidelity of this conversion, with differ-  
116 ent conversion factors for at-sea, off-sea, off-land and in-land parts of the storm suggested (Harper  
117 et al. 2010). Other uncertainties also exist in the best track data, which have been discussed in  
118 several studies; a summary of these uncertainties can be found in the appendix of Hodges and

119 Emerton (2015). They include issues relating to location and intensity uncertainties and opera-  
120 tional differences between agencies. This is further discussed in the Discussion section.

121 For the analysis of the identified TCs in different ocean basins the IBTrACS basin boundaries  
122 (Knapp et al. 2010) have been used, with TCs assigned to a particular ocean basin, based on where  
123 the storm reaches maximum wind speed intensity.

#### 124 *b. Reanalysis datasets*

125 Meteorological centers around the world produce reanalysis data sets as an ongoing enterprise.  
126 The reanalyses are essentially based on frozen operational numerical weather prediction (NWP)  
127 systems. New reanalyses are often released following significant improvements in the models  
128 and data assimilation schemes. The reanalyses differ in terms of the models and data assimi-  
129 lation methods used to produce them, therefore differences in their output are to be expected. Six  
130 recent global atmospheric reanalysis data sets have been analysed for TCs in this study and are  
131 summarized in Table 1. They include the European Centre for Medium-Range Weather Forecasts  
132 (ECMWF) Interim reanalysis (ERA-Interim) (Dee et al. 2011); the Japanese 25-year reanalysis (JRA25)  
133 (Onogi et al. 2007) and 55-year reanalysis (JRA55) (Kobayashi et al. 2015); the National Aero-  
134 nautics and Space Administration (NASA) Modern-era Retrospective Analysis for Research and  
135 Applications (MERRA) (Rienecker and coauthors 2011) and the following version 2 (MERRA2)  
136 (Bosilovich and coauthors 2015; Molod et al. 2015); and the National Centers for Environmental  
137 Prediction (NCEP) Climate Forecast System Reanalysis (NCEP-CFSR) (Suranjana and Coauthors  
138 2010). The NCEP-CFSR reanalysis is the only coupled atmosphere-ocean-land surface-sea ice  
139 reanalysis. The NCEP-CFSR, MERRA and MERRA2 all use different versions of the 3D vari-  
140 ational (3D-Var) data assimilation scheme: the Grid-point Statistical Interpolation (GSI) scheme  
141 (Shao et al. 2016). For MERRA and MERRA2 the Incremental Analysis Update (IAU) (Bloom

142 et al. 1996; Rienecker and coauthors 2011) system is also used. The data period used for all the  
143 reanalyses is 1979-2012, except for MERRA2, which starts in 1980. A key difference between the  
144 JMA reanalyses and the reanalyses produced by the other agencies is the assimilation of tropical  
145 wind retrievals (TWR). Wind profile data over and around tropical cyclone centers are retrieved  
146 from historical data and processed and assimilated as if they were dropsonde observations (Hat-  
147 sushika et al. 2006). With the integration of this additional wind data, the intensity of the storms  
148 in the JMA reanalyses is found to be improved (Hatsushika et al. 2006). Another difference be-  
149 tween the reanalyses is that the NCEP-CFSR uses a technique to improve the representation of  
150 TCs by adjusting the location of the tropical vortex to its observed location before the assimilation  
151 of storm circulation observations (Suranjana and Coauthors 2010). The MERRA2 reanalysis also  
152 uses this method. All the reanalyses in this study make use of quality control processes and bias  
153 correction for the diverse range of observations that are assimilated, for example, the variational  
154 bias correction of satellite radiances (Dee and Uppala 2009).

### 155 *c. Tropical cyclone detection method*

156 The analysis of TCs in this study relies on identifying and tracking them. The first step is to track  
157 all tropical disturbances, in both hemispheres, before applying two different identification methods  
158 to separate the TCs from other tropical systems. This is different from some other schemes where  
159 the identification is performed during the tracking and hence only identifies the TC stage of the  
160 lifecycle. Though not crucial to this study, the approach taken here identifies much more of the  
161 lifecycle, including the precursor and post extratropical transition stages (Jones et al. 2003).

162 For the first step, where all systems in the domain are tracked, the tracking methodology is based  
163 on Hodges (1994, 1995, 1999). The domain extends to 60N in the NH and 60S in the SH. The  
164 tracking method uses the 6 hourly relative vorticity at the levels 850, 700, 600hPa, vertically aver-

aged. This data is spectrally filtered using triangular truncation to retain total wavenumbers 6-63. The spectral coefficients are also tapered to further smooth the data using the filter described in Sardeshmukh and Hoskins (1984). The spectral filtering acts to remove the noise associated with the smallest spatial scales in the vorticity, which produces more reliable tracking in data of this type, and to remove the large scale background, which is also found to be beneficial. The tracking proceeds by identifying the off-grid vorticity maxima, by applying a maximisation scheme (Hodges 1995), that exceed a value of  $5 \times 10^{-6} s^{-1}$  in each time frame (SH scaled by -1). These are initially linked together using a nearest neighbor approach and then refined by minimizing a cost function for track smoothness, subject to adaptive constraints on displacement distance and track smoothness (Hodges 1999). The use of the vertically averaged vorticity is different from some previous studies using this tracking algorithm, where the single level of 850hPa vorticity reduced to T42 resolution was used (Strachan et al. 2013; Roberts et al. 2015; Bell et al. 2013; Bengtsson et al. 2007b; Manganello et al. 2012). The use of the vertically averaged vorticity is found to improve the temporal coherency when a vorticity maximum shifts between levels (Serra et al. 2010; Fine et al. 2016) and results in more of the system lifecycle being detected. A simple vertical average is found to be sufficient, even though the levels are not evenly spaced, since, once spectrally filtered, there is little difference from using the mass weighted vertical average. Only tracks that last at least 2 days (8 time steps) are retained for further analysis. Whilst observed TCs can have lifetimes shorter than 2 days, this only covers the period when they are determined to be TCs, whereas the tracking scheme used here aims to identify the precursor and post-TC stages resulting in much longer lifetimes (see Figure 1c and d) so that using the 2 day threshold is not detrimental to detecting nearly all the observed TCs in the reanalyses, as shown below in the results section.

188 Previous methods used to detect TCs in reanalysis or GCM data rely on applying particular cri-  
189 teria, representative of the properties of TCs, such as some thresholds on intensity, e.g. Mean Sea  
190 Level Pressure (MSLP) minima, low level wind intensities or vorticity extrema, and a threshold  
191 on the warm core structure either determined directly as a temperature anomaly, or inferred from  
192 the presence of decreasing winds or vorticity between the lower and upper troposphere, for exam-  
193 ple Bengtsson et al. (1995) and related methods. These are often applied as part of the tracking  
194 scheme itself, which is different from the approach used here. A minimum period of one day is  
195 typically imposed, for which these criteria are satisfied contiguously, and that they are satisfied  
196 only over the ocean by imposing the land-sea mask. The criteria based on intensity and structure  
197 can be strongly dependent on the model resolution and how processes important to TC devel-  
198 opment, such as convection, microphysics and surface drag, are represented in the model. This  
199 has resulted in some studies using resolution dependent identification criteria (Walsh et al. 2007;  
200 Manganello et al. 2012) or tuning the identification criteria to maximize the detected TCs, for ex-  
201 ample in reanalyses compared with observations (Murakami 2014), and some studies have used  
202 basin dependent criteria (Camargo et al. 2005). The study of Horn et al. (2014) has shown that the  
203 subjective choice of different identification criteria is the main reason for differences between the  
204 numbers of TCs identified by different identification schemes.

205 In this study a dual approach is taken to isolate the TCs from all the tracked systems. Taking  
206 the tracks identified in the first stage, where all systems are tracked, the first approach used to  
207 isolate the TCs is used to see which of the observed TCs in the IBTrACS data set can be found in  
208 the reanalyses, without applying any criteria dependent on intensity or structure. This approach  
209 makes use of spatio-temporal matching: a track in the reanalyses matches with a track in IBTrACS  
210 if the mean separation distance between them, computed over the time period that they overlap, is  
211 less than  $4^0$  (geodesic), and is the least mean separation distance if more than one track satisfies

212 this criterion, where any amount of temporal overlap is allowed. This will be termed the "di-  
213 rect matching" method. A similar approach has previously been used for extra-tropical cyclones  
214 (Hodges et al. 2003). The relaxed criterion on the temporal overlap is chosen because, in general,  
215 the TCs in IBTrACS have much shorter lifetimes compared to the tracks in the reanalyses pro-  
216 duced by the tracking scheme. Several diagnostics are produced from the matched tracks, such as  
217 the mean separation distance distribution, lifetime distribution and intensity distribution based on  
218 low level winds, 10m and 925hPa, and MSLP.

219 The second approach used to isolate the TCs from all the tracked systems is to objectively  
220 identify them using a typical set of identification criteria based on intensity and structure; this will  
221 be termed the "objective detection" method. The criteria used are similar to those used previously  
222 with this tracking algorithm (Bengtsson et al. 2007a,b; Strachan et al. 2013). This requires adding  
223 additional fields to the tracks, namely the T63 vorticity at levels 850, 700-200hPa to provide  
224 intensity and warm core criteria. This is done by recursively searching for a vorticity maximum  
225 at the different levels using the maximum at the previous level as a starting point for a steepest  
226 ascent maximization applied to the B-spline interpolated field. A search radius of  $5^{\circ}$  (geodesic)  
227 is used centered on the location at the previous level. The same approach is used in the Southern  
228 Hemisphere (SH) by multiplying fields by -1. Also added are the Mean Sea Level Pressure (MSLP)  
229 minimum and maximum winds at 10m and 925hPa as alternative measures of TC intensity. For  
230 MSLP a steepest descent method is used with the B-spline interpolation and a search radius of  $5^{\circ}$   
231 (geodesic) centered on the tracked vorticity center to find the closest pressure minimum, whilst  
232 for the winds a direct search for the maximum winds within  $6^{\circ}$  of the tracked center is used. The  
233 criteria for identification are:

- 234 1. the T63 relative vorticity at 850 hPa must attain a threshold of at least  $6 \times 10^{-5} s^{-1}$ .

- 235 2. the difference in vorticity between 850 and 200 hPa (at T63 resolution) must be greater than  
236  $6 \times 10^{-5} s^{-1}$  to provide evidence of a warm core.
- 237 3. the T63 vorticity center must exist at each level between 850 and 200hPa for a coherent  
238 vertical structure.
- 239 4. criteria (1) to (3) must be jointly attained for a minimum of 4 consecutive time steps (one  
240 day) and only apply over the oceans.
- 241 5. tracks must start within 30S to 30N.

242 The approach used here means that the tracking and identification is performed at a common  
243 resolution for all the reanalyses, making the tracking and identification as resolution independent  
244 as possible, although the actual model resolution will still have some impact on the identification.

245 The TCs identified by the objective detection method are also matched against the observed  
246 tracks in IBTrACS, using the same criteria as in the direct matching method, to determine the hit  
247 and miss rates of the identification scheme.

248 The tracking is applied to each full year, January-December, for the Northern Hemisphere (NH)  
249 and July to June the following year in the Southern Hemisphere (SH), resulting in 34 years in the  
250 NH and 33 in the SH (33 and 32 respectively for MERRA2).

### 251 **3. Results**

252 In this section the ability of the different reanalyses to simulate different aspects of TC behavior  
253 is assessed and compared to the observed TC activity, as represented by the IBTrACS database  
254 described in the Best Track dataset subsection.

255 *a. Direct Matching Results*

256 The number of TCs in IBTrACS that match with a storm in the reanalyses for each reanalysis  
257 using the direct matching method are summarized in Table 2 for both NH and SH. This shows that  
258  $\sim 95\%$  of the TCs in IBTrACS are identified in the reanalyses in the NH and  $\sim 92\%$  in the SH.  
259 The different reanalyses are remarkably similar in this respect. In general the TCs not found in the  
260 analyses tend to be the weakest and/or short lived TCs in IBTrACS in both hemispheres. Some of  
261 the missing TCs fail to pass the 2 day lifetime threshold imposed on the reanalysis tracks. There is  
262 also some evidence that the number of missing TCs in the reanalyses, according to the matching  
263 criteria, are reduced in the later period after 2000: compared to the earlier period, the number of  
264 matches increases to  $\sim 98\%$  in both NH and SH. This improvement may be associated with the  
265 assimilation of improved observations, in particular the availability of surface scatterometer winds  
266 from the QuikSCAT satellite data from mid-1999 until the end of 2009 and continuing with similar  
267 data from other remote sensing platforms since then.

268 To see how the TCs identified in the reanalyses by the direct matching method compare with  
269 those in IBTrACS several sets of statistics are produced.

270 1) LOCATION

271 Figure 1a and b show distributions for the mean separation distance (geodesic distance) between  
272 the identical reanalysis tracks and those of IBTrACS, obtained using the direct matching method,  
273 in the NH and SH respectively. In the NH (Figure 1a) the majority of TCs identified in the re-  
274 analyses have a mean separation from those in IBTrACS of less than  $2^0$  ( 220km), with the peak  
275 of the distribution for each reanalysis typically at less than  $1^0$  ( 110km). The smallest mean sep-  
276 aration distances occur for JRA55, with the distribution peak at  $0.5^0$  (56km) and the largest for  
277 MERRA, with the distribution peak at  $1^0$  and the other reanalysis somewhere in between. The

278 JRA55 separation distances are comparable with those from the much higher resolution (T1279;  
279 16km)) operational analyses of ECMWF (Hodges and Emerton 2015) (Appendix), which may be  
280 a consequence of the assimilation of the TWR observations in JRA55. This conjecture is strength-  
281 ened by the fact that JRA25, which also assimilates TWR data, is comparable in terms of the mean  
282 separation distances to the much higher resolution NCEP-CFSR reanalysis. It is also apparent that  
283 MERRA2 has improved over MERRA with respect to the separation distances. In general the  
284 mean separation results for the NH (Figure 1a) are consistent with those found by Schenkel and  
285 Hart (2012) for the identical reanalyses considered. In the SH (Figure 1b) a rather similar picture  
286 is seen, with each of the reanalyses occurring in the same order as in the NH of best to worse.  
287 Whilst the separation distances appear slightly larger for some reanalyses in the SH, i.e. ERAI and  
288 MERRA, the others are comparable with the results in the NH, highlighting the improvement in  
289 the SH in the more recent reanalyses compared with older reanalyses.

## 290 2) LIFETIME

291 Figure 1c and d show the lifetime distributions in the NH and SH respectively. In the NH it is  
292 apparent that the TCs identified in the reanalyses have much longer lifetimes than the TCs in the  
293 observations. This is a consequence of not imposing any criteria during the tracking to identify  
294 TCs. Imposing the TC detection criteria during the tracking would truncate the tracks to the TC  
295 stage alone, and would introduce a dependency of the lifetime on the chosen criteria and how well  
296 TCs are represented in the reanalyses in terms of intensity and structure. The extended lifecycles  
297 include pre-TC stages, e.g. easterly waves and the stage after extratropical transition. Some of  
298 the reanalysis TCs can exist for longer than one month, in which time a precursor disturbance  
299 can travel across an ocean basin, develop into a TC and recurve to high latitudes undergoing  
300 extratropical transition, whereas none of the observed TC tracks last this long. The distributions for

301 the different reanalyses are quite close together, showing that rather similar lifetimes are obtained  
302 for all the reanalyses. A similar set of results is obtained in the SH, although the distributions for  
303 the reanalyses are a little noisier, due to the smaller number of observed TCs in this hemisphere.

### 304 3) LATITUDE OF MAXIMUM INTENSITY

305 The latitude at which the maximum intensity is attained in terms of the 10m winds is shown for  
306 the NH and SH in Figure 1e and f respectively. In the NH the distributions show that, whilst most  
307 TCs in the reanalyses attain their maximum intensity at similar latitudes to those in the observa-  
308 tions, there are some TCs that attain their maximum intensity at much higher latitudes. A possible  
309 cause for this behavior is that, because of the longer lifecycles that are identified in the reanalyses,  
310 some storms only attain their maximum intensity as they recurve to higher latitudes and become  
311 larger and better represented at synoptic scales. Whilst this could be addressed by restricting the  
312 reanalysis tracks to just the TC stage, this would mean either truncating the tracks where they  
313 overlap with the best track data (Hodges and Emerton 2015), or using the detection criteria based  
314 on intensity and structure discussed above to define the TC part of the lifecycle. Either of these  
315 approaches introduces a degree of subjectivity: the first as it depends on the different operational  
316 practices of the operational agencies, and the second because it depends on how well TCs are rep-  
317 resented in the different reanalyses. Also, for this part of the study, we want to see what exactly is  
318 in the reanalyses in terms of TC lifecycle and restricting the lifecycles defeats this objective. This  
319 is also important for future work, such as studies of extratropical transition and risk associated with  
320 TCs and their later lifecycle stages in extratropical regions. A similar situation may also occur for  
321 the TC stage itself, where the relatively low resolution of the reanalyses means that TCs are not  
322 well represented at the small spatial scales of TCs in the tropics, but become better represented  
323 as they move to higher latitudes. A similar picture is seen for the SH (Figure 1f). This type of

324 behaviour is often seen for TCs identified in relatively low resolution climate model simulations  
325 (Manganello et al. 2012).

#### 326 4) INTENSITY

327 Also examined are the maximum intensity distributions of the TCs for three intensity measures:  
328 minimum MSLP and maximum 10m and 92hPa wind speeds, which are shown in Figure 2 for  
329 both NH and SH TCs. For both MSLP (Figure 2a, b) and 10m wind speeds (Figure 2c, d) in the  
330 NH and SH it is clear that all the reanalyses underestimate the intensity of TCs compared to the  
331 observations and that the intensities are model dependent. This is not surprising considering the  
332 relatively low spatial resolutions of the reanalyses where the assimilation of observations cannot  
333 correct for this. Previous studies with dynamical downscaling of individual historical TCs, such  
334 as Katrina, have shown that resolutions  $\sim 1\text{-}5\text{km}$  with a non-hydrostatic model are necessary to  
335 simulate TC inner-core processes correctly in order to enable the right magnitude of wind inten-  
336 sities (Davis et al. 2008) to be simulated. However, some studies using hydrostatic models with  
337 parameterized convection at resolutions  $\sim 10\text{km}$  can certainly produce TCs with depths as large  
338 if not larger than observed (Manganello et al. 2012). Coupling to the ocean has also been found  
339 to be important in correctly simulating TC intensity (Kilic and Raible 2013), although only the  
340 NCEP-CFSR reanalysis applies any such coupling and its impact on the reanalysis and TCs is  
341 uncertain.

342 The results for intensity based on the MSLP (Figure 2a, b) show that in general the more recent  
343 reanalyses, NCEP-CFSR, JRA55 and MERRA2 have deeper TCs; this is more evident in the SH,  
344 although in both hemispheres few TCs reach depths below 940hPa. The more recent reanalyses  
345 may be performing slightly better with respect to this intensity measure, possibly due to better  
346 use of the available observations and improved models, and not necessarily due to resolution. For

347 10m wind speeds (Figure 2c, d), much larger differences are seen between the different reanal-  
348 yses, although, as already mentioned, none of them can simulate the strongest intensities seen  
349 in the observations. NCEP-CFSR has the most intense TCs in terms of 10m wind speeds, with  
350 some TC almost attaining intensities of  $50 \text{ ms}^{-1}$  (Category 3 TS) but with no Category 4 or 5  
351 (Saffir-Simpson scale) TSs. The weakest maximum 10m wind speed intensities are produced by  
352 the MERRA reanalysis with no TCs surpassing  $30 \text{ ms}^{-1}$ , which barely reaches Category 1 TS.  
353 However, the more recent MERRA2 reanalysis shows a significant improvement being compara-  
354 ble with the JRA55 reanalysis in having TCs that can almost attain 10m wind speeds of  $40 \text{ ms}^{-1}$   
355 (Category 1 TS), although less than that seen for the NCEP-CFSR reanalysis. The results for the  
356 reanalyses TC 10m wind speeds show similar behavior in both hemispheres. The results for both  
357 10m wind and MSLP maximum intensities are generally consistent with those of Schenkel and  
358 Hart (2012) for the NH. One problem with using the 10m winds from the reanalyses is that they  
359 are not a direct model prognostic field, but are computed as a diagnostic, though not necessarily  
360 in the same way for each reanalysis. They are generally computed as an extrapolation from the  
361 lowest model level to the surface using profile functions and corrected when over land for terrain  
362 roughness to conform to the World Meteorological Organization (WMO) standard for SYNOP  
363 observations (for example see, ECMWF (2015)). However, for some reanalyses this is not done  
364 for the actual analyses: for example in MERRA, it is performed during the IAU cycle, so does not  
365 see the full analysis increment, and is an average over four model time steps (private communica-  
366 tion, Michael Bosilovich, NASA). To evaluate the uncertainty further, the maximum wind speeds  
367 at the 925hPa pressure level associated with the TCs are also considered (pressure level winds are  
368 obtained by interpolation between model levels); the TC 925hPa winds are shown in Figure 2e,  
369 f for the NH and SH respectively. The downside to using the 925hPa winds is that there are no  
370 available observations with which to compare with, although this is not critical here, where we

371 just want to see if the same differences between the reanalyses, as seen for 10m winds, occur at  
372 this level. The results for the wind speed intensity at 925hPa show a rather different perspective  
373 from those at 10m, with both NCEP-CFSR and MERRA2 having comparable values in the tail of  
374 the distribution with values as high as  $60 \text{ ms}^{-1}$ . The MERRA reanalysis is now comparable with  
375 the other reanalyses of JRA55, JRA25 and ERAI.

## 376 5) WIND SPEED-PRESSURE RELATIONSHIP

377 The wind speed-pressure relationship is often used by the operational centers to estimate winds  
378 from pressure measurements and surface pressure from wind measurements, for which various  
379 quadratic empirical relationships have been developed based on cyclostrophic balance (Knaff and  
380 Zehr 2007). Hence, the wind-pressure relationship of TCs is often considered in studies of TCs in  
381 models and reanalyses (Roberts et al. 2015) to compare with the observed relationship, although  
382 it should be noted that the observations may themselves be estimated from one of the empirical  
383 relationships, which can differ between agencies (Knaff and Zehr 2007). Figure 3a shows the  
384 wind-pressure relationship for the observations and the TCs identified in the different reanalyses  
385 using the direct matching method in the NH. The wind-pressure relationship is determined using  
386 the 10m wind speeds and MSLP values, by determining the maximum attained 10m wind speed  
387 and taking the MSLP value at the same time. The results show that all the reanalysis reflect  
388 the underestimate of both the 10m wind speeds and MSLP depths of the TCs, this being most  
389 prominent for MERRA. This can be related to the radius of maximum wind (RMW), computed for  
390 the reanalyses at the time of maximum 10m wind intensity, and shown for the NH in Figure 3c. The  
391 RMW is not available for all the agencies in IBTrACS but we estimate it at the time of maximum  
392 wind intensity, based on the simple Rankine model described by Knaff and Zehr (2007), this gives  
393 RMW values for the observations predominately below  $\sim 100\text{km}$  ( $1^0$ ) and a peak around  $\sim 50\text{km}$

394 (0.5<sup>0</sup>). This is consistent with the findings of Kimball and Mulekar (2004) for North Atlantic TSs  
395 who made use of an extended "best track" data set. For all the reanalyses the RMW are seen to be  
396 too large (Figure 3c). Assuming gradient wind balance for the TCs, and the fact that RMWs are  
397 too large and wind intensities are too low for the reanalyses implies that the pressure difference  
398 between the storm centers and the environment is also too low, consistent with the wind speed-  
399 pressure relationship in Figure 3a. The fact that the NCEP-CFSR has the strongest wind intensities  
400 and one of the smallest RMWs is also consistent with the result in Figure 3a that NCEP-CFSR is  
401 closest to the observed wind speed-pressure relationship, whereas MERRA, which has the weakest  
402 maximum wind speeds and large RMWs, is the worst of the reanalyses in this respect. MERRA2  
403 shows a significant improvement over MERRA in terms of the wind speed-pressure relationship  
404 which can be understood in terms of the improved maximum wind speeds and lower RMWs. In  
405 fact, MERRA2 has the lowest RMWs, although is not as strong in intensity (10m wind speed) as  
406 NCEP-CFSR.

407 The fact that NCEP-CFSR appears to perform the best in terms of the wind speed-pressure rela-  
408 tionship may be the result of the vortex relocation scheme used by the NCEP-CFSR assimilation  
409 system, which, as pointed out by Schenkel and Hart (2012), will result in improved vortex location,  
410 which in turn may lead to improved TC intensities as a result of the TC being in the correct envi-  
411 ronment. Allied to this, Schenkel and Hart (2012) also pointed out that observations within the TC  
412 vicinity are less likely to be rejected by the assimilation scheme, due to smaller differences with  
413 the first-guess field. However, the situation is likely more complex than this, as MERRA2 also  
414 uses the vortex relocation method and has the lowest RMWs but is not the most intense in terms  
415 of wind speed. JRA55, on the other hand, with a similar resolution to MERRA2, has the smallest  
416 location errors (Figure 1a, b), does not use vortex relocation, but does assimilate best track data as  
417 synthetic dropsondes (Hatsushika et al. 2006) and has comparable intensities to MERRA2 and a

418 wind speed-pressure relationship, also very similar to MERRA2. Hence, it appears that there are  
419 complex trade-offs occurring within the assimilation systems. In the SH the wind-speed pressure  
420 relationship (Figure 3b) and RMWs (Figure 3d) appear to be very similar to those in the NH: in  
421 particular the wind-speed pressure relationship appears to be closely associated with the ordering  
422 of the 10m wind speeds of the reanalyses shown in Figure 2b.

#### 423 *b. Objective Identification*

424 Following the assessment of how well TCs are represented in the chosen reanalyses it is of  
425 interest to see how existing objective TC identification schemes perform in order to try and un-  
426 derstand the impacts of the differences between reanalyses on objective TC identification. This  
427 is important, as objective schemes are the only way to identify TCs in climate model simulations  
428 and they are often contrasted with reanalyses as a means of verification at comparable resolutions.  
429 As Murakami (2014) has shown, detection schemes have to be tuned to particular reanalyses to  
430 optimally detect TC/TS frequencies. This is also what tends to happen in operational settings,  
431 where detection schemes are often tuned to a particular operational setup, so that applying them to  
432 data from a different operational center can give very different numbers of detected TCs from the  
433 in-house method (c.f. Fig. 22 of Kobayashi et al. (2015)). Some schemes also adjust identification  
434 criteria by ocean basin (Camargo and Zebiak 2002) to account for model biases. However, these  
435 are not appealing approaches in the climate model context, where a fixed set of criteria, applied in  
436 a common resolution framework, will provide a better comparison between different model sim-  
437 ulations or different climate scenarios (Shaevitz and Coauthors 2014). To assess how one such  
438 scheme performs, the objective detection method described in the methodology section, based on  
439 the vorticity at multiple levels between 850 and 200hPa, is applied to the vorticity tracks obtained  
440 from the tracking of all vorticity centres.

## 441 1) ANNUAL COUNTS

442 The annual average TC counts are determined for each ocean basin (Figure 4) and are shown in  
443 Figure 5. In the NH the annual number is in reasonably good agreement with the observations of  
444 IBTrACS apart from MERRA, which has  $\sim 30$  fewer identified TCs, whilst the other reanalyses  
445 are slightly over or under in number, a result also previously noted by Murakami (2014) using the  
446 same criteria. However, in the SH the identification has resulted in a much higher number than in  
447 the observations, which occurs for all the ocean basins. The overestimation is particularly large  
448 in the South Pacific (SP) region; the South Atlantic (SA) region also has more identified systems  
449 than are in the observations. These differences will be discussed further in the Discussion section.

## 450 2) MATCHING AGAINST IBTRACS

451 To further analyse the objectively identified TCs, they are matched against the observed TCs of  
452 IBTrACS using the direct matching method to identify the common storms between the two and  
453 the false positive and negative detections. The results of this track matching are shown in Table 2  
454 in terms of the Probability of Detection (POD) and False Alarm Rate (FAR). The POD is defined  
455 here as the number of matched storms for each reanalysis divided by the total number of storms in  
456 the observations, and the FAR by the number of non-matched storms in each reanalyses divided  
457 by the total number of storms in the same reanalysis. Also shown in Table 2, for comparison, are  
458 the POD for the direct matching results, before applying the objective criteria, discussed in the  
459 Direct Matching Results subsection, which shows an almost uniform detection rate of 0.95 across  
460 all the reanalyses in both hemispheres, although this is lower in the SH than the NH. The reason  
461 why the POD for the SH is lower for the pre-criteria matching is likely related to differences in  
462 the observations that are assimilated in the reanalyses between the two hemispheres, as there is no  
463 dependence on structure or intensity for detection for these results.

464 For the POD based on using the objective detection method the values are much lower, with the  
465 best detection for JRA55 and the worst for MERRA in both hemispheres, although POD is higher  
466 in the SH than the NH, possibly due to differences in sample sizes. The FAR (Table 2) shows  
467 values ranging from 0.16 for JRA25 to 0.36 for NCEP-CFSR in the NH. The fact that JRA25 has  
468 the lowest FAR may be related to this reanalysis having the lowest resolution, hence, detecting  
469 fewer small scale and possibly weaker storms; this could be investigated using GCMs of varying  
470 resolution. In the SH, FAR is much higher, as might be expected from the previous discussion, due  
471 mostly to the higher number of TCs detected compared with the observations. From these values  
472 of POD and FAR it is apparent that, although similar numbers of TCs are detected in the NH using  
473 the objective detection method, they need not be identical to the ones in the observations.

474 To explore the POD and FAR values in more detail the storms that are in the observations and that  
475 match and do not match with those identified in the re-analyses, using both identification methods,  
476 pre-objective direct matching and post-objective matching, are further analyzed relative to their  
477 attained category in the observations according to the Saffir-Simpson scale determined from the  
478 1min. observed winds. Hence, the IBTrACS storms are partitioned into the categories according to  
479 the 1min. winds before matching them against the reanalysis tracks, as previously described. Since  
480 different agencies use different wind intensity scales, this approach provides a more consistent  
481 classification across the different ocean basins. Since some weak storms in IBTrACS have no wind  
482 information, they are excluded from this analysis; Murakami (2014) excluded tropical depressions  
483 from their study, although it is unclear how this is achieved for the reanalyses, apart from applying  
484 the agency wind thresholds. The results of this analysis by category are shown in Tables 3 and  
485 4 for the NH and SH respectively. In the NH, Table 3 shows that for the objectively identified  
486 TCs it is the weakest categories that have the poorest level of matches between the reanalyses  
487 and IBTrACS, in particular for the tropical depressions, although many tropical depressions in

488 IBTrACS are excluded due to lack of wind information. However, for the TS category (between  
489 tropical depression and Category 1) the best performing reanalyses at this level, JRA25 and JRA55,  
490 match with 78.5% of IBTrACS storms, while for the worst performing (MERRA) only 41.6% of  
491 IBTrACS storms match. For the higher TS wind speed categories the percentage of matches  
492 with IBTrACS steadily increases with category on progressively smaller sample sizes, i.e. 92%,  
493 98%, 99.5% and 100% for CAT1-CAT5 respectively, for the best performing JRA25 and JRA55  
494 and considerably worse for MERRA (63.5, 75, 83, 82.5, 92%) with NCEP-CFSR and MERRA2  
495 comparable with JRA25 and JRA55. Re-calculating the POD for just Cat1-Cat5 TS (Table 5) the  
496 best performing reanalyses, JRA25 and JRA55 now have values 0.95.

497 In the SH, Table 4 shows that a fairly similar situation occurs as in the NH for the objectively  
498 identified TCs, except that it is apparent there are virtually no tropical depressions available to  
499 compare with in the observations, either because very few of this category of storms have any  
500 wind values, or more likely that they are not generally included in the best track data sets in this  
501 hemisphere; this is discussed further in the discussion section. The best degree of matches again  
502 occurs for the JRA25 and JRA55, ranging from 84-89% for the weakest TSs (TS Category) to  
503 95% for CAT5.

504 The POD, for CAT1-CAT5 objectively identified TS only, shown in Table 5, shows that for this  
505 intensity range the values are comparable in both hemispheres and comparable with the results  
506 in the study of Murakami (2014) who restricted their study to this intensity range, although they  
507 used different skill metrics compared to here and in the study here there is no special tuning of the  
508 objective detection parameters for each reanalysis as in Murakami (2014).

509 For the TCs identified using the direct matching method (pre-objective), previously discussed  
510 in the Direct Matching Results subsection, the matching by observation category (not shown)

511 indicates consistently high POD values as reported in the Direct Matching Results subsection for  
512 all categories and reanalyses.

513 To understand the nature of the TCs, identified by the objective detection method, in the reanal-  
514 yses that do not match with the IBTrACS TCs, in particular in the SH, those that do not match are  
515 binned according to the latitude of their genesis. For the SH this is shown in Figure 6(a). This  
516 shows essentially two groups of storms: those with genesis within 0-20S and those with genesis  
517 occurring south of 20S. The genesis for all TCs in IBTrACS is almost entirely within 0-20S (not  
518 shown). Examining these two groups on non-matching objectively identified TCs separately, a  
519 scan of the tropical storm advisories (discussed later) indicates that some of the identified storms  
520 in the first group can be found in the advisories but not IBTrACS; this is discussed further in the  
521 Discussion section. Figure 6(b) shows examples of two tracks identified in ERAI that do not match  
522 with IBTrACS: the track labeled "Storm 1" occurs in January of 2011 and is a storm that possibly  
523 occurs in the RMSC Nadi advisories, named 02F, but is not in IBTrACS, probably because it did  
524 not develop further into a true TS. Even so, it seems a substantial storm with 10m winds in ERAI  
525 over  $20 \text{ m s}^{-1}$  whilst near Australia. Figure 6(c) shows the infrared satellite image, which presents  
526 an asymmetric structure, unlike a true TS, with this storm more likely to be a hybrid warm core  
527 TC. The second storm shown in Figure 6(b) originates south of 20S, where very few IBTrACS  
528 storms have their genesis. This particular storm seems to have formed in the vicinity of the South  
529 Pacific Convergence Zone (SPCZ) and travels south eastward with relatively weak 10m winds in  
530 ERAI  $\sim 15 \text{ m s}^{-1}$  through a region of very little habitable land. It has no reference in any tropical  
531 storm advisories, yet its structure in the satellite imagery (Figure 6(d) shows some similarities with  
532 "Storm 1" (Figure 6(c)) and it may also be a hybrid TC. As shown by Yanase et al. (2014) (Figure  
533 1) using the Hart phase space classification of cyclones (Hart 2003), applied to reanalysis data,  
534 storms found between 20-40S in the SH summer tend to be hybrid storms. There are also storms

535 in IBTrACS that do not match with an analysis track, but these tend to be the weakest storms  
536 below Category 1 as shown in Tables 3 and 4. These issues are further discussed in the Discussion  
537 section.

#### 538 **4. Discussion**

539 There are several possibilities for the poorer performance of the objective detection method in  
540 the SH compared with the NH in terms of the detection, relative to the observed TCs in IBTrACS.  
541 As shown above, the discrepancy in numbers is closely associated with the weakest storms, trop-  
542 ical depressions and tropical storms (below Category 1). The first possibility for the differences  
543 between the NH and SH objective detection may be due to different biases in the best track data  
544 in the SH compared with the NH; the second is due to different biases in the representation of  
545 TCs in the reanalyses between the NH and SH; the third is due to the selection criteria used by the  
546 objective detection method to identify TCs in the reanalyses being not selective enough, or being  
547 mainly tuned to the NH. These will be addressed in turn.

548 In terms of possible biases in the IBTrACS observations, it is possible that the SH is observed  
549 differently than in the NH. The SH is sparsely inhabited in particular regions, such as the SP and  
550 SA, so that less emphasis may be placed on detection except for the most intense systems likely  
551 to make landfall (Kucas et al. 2014). Related to this is the application of different storm detection  
552 procedures in the different warning centers that produce the best track data (Velden and Coauthors  
553 2006b; Kueh 2012). Storm classification is primarily based on the interpretation of satellite obser-  
554 vations using empirical relationships such as the Dvorak scheme (Velden and Coauthors 2006a);  
555 there is little aircraft reconnaissance apart for the North Atlantic with some other limited cover-  
556 age associated with field campaigns and in specific regions, e.g. Taiwan (DOTSTAR) (Wu and  
557 Coauthors 2005). The uncertainties of applying operational detection and classification schemes

558 when storms are relatively weak and show a poor organization (Torn and Snyder 2012) may make  
559 deciding between whether a tropical disturbance should be classified as a tropical depression and  
560 counted in best track, or is some other tropical storm such as a subtropical or hybrid cyclone, dif-  
561 ficult and dependent on subjective forecaster interpretation. Gyakum (2011) states that "there is  
562 presently no single set of objective criteria that, if applied operationally, would irrefutably support  
563 a forecasters analysis of cyclone type (subtropical, hybrid or tropical)". It is also unclear whether  
564 all agencies report weaker storms such as tropical depressions consistently in their best track anal-  
565 yses, and hence whether they make their way into IBTrACS. For example, HURDAT, produced by  
566 the National Hurricane Center (NHC), and which forms part of IBTrACS, and covers the North At-  
567 lantic and North Eastern Pacific includes subtropical cyclones (Landsea and Franklin 2013) where  
568 as the Joint Typhoon Warning Center (JTWC), which covers the Western North Pacific, South  
569 Pacific and South and North Indian Oceans, do not routinely include subtropical cyclones (Kucas  
570 et al. 2014; Gyakum 2011) unless they undergo Tropical Transition (TT) (Bentley et al. 2016;  
571 McTaggart-Cowan et al. 2013). Even within a single ocean basin where multiple agencies are op-  
572 erational, considerable uncertainties exist between different best track data sets. For example, Ren  
573 et al. (2011) and Barcikowska et al. (2012), highlight significant differences between JTWC and  
574 Japan Meteorological Agency (JMA) best track data in the Western North Pacific (WNP) in terms  
575 of frequency and intensity of TCs, with better agreement for frequencies for Category 2 TS and  
576 above; this is exactly where our objective detection scheme performs best in both hemispheres.

577 Therefore, uncertainties in the interpretation of the observations for the weaker tropical storms,  
578 and different agency operational procedures, may result in their exclusion from the best track  
579 archive. Several reassessments of best track data, in particular in the SH, have resulted in the inclu-  
580 sion of some additional storms, but also the removal of some others (Diamond et al. 2012) so that  
581 actual numbers are not significantly changed. However, evidence that the SH may be being treated

582 differently for tropical storms in the observations than in the NH, in particular with respect to the  
583 weaker sub-tropical and hybrid storms, can be seen by considering the tropical storm advisories.  
584 Information on weak tropical disturbances, together with TCs, is available in text based reports  
585 from the warning agencies, such as the JTWC "significant tropical cyclone advisories". However,  
586 not all this information is included in the best track post season analysis and hence IBTrACS.  
587 For example, in the South Pacific, IBTrACS reports 5 storms in the 2011/2012 season (July-June)  
588 but scanning the advisories (Regional Specialized Meteorological Center (RSMC) Nadi) results  
589 in a much larger number of tropical disturbances,  $\sim 20$ . A more quantitative comparison can be  
590 made using the combined advisories from each warning center, for each year, in each hemisphere  
591 (July-June in the SH). This information has been collated by Padgett and Young (2016) from 1998  
592 onwards for both hemispheres, although some very weak systems are not included. Comparing  
593 the numbers in the advisories with those in IBTrACS over the period 1998-2012, which overlaps  
594 with our study period; in the NH, IBTrACS has on average 69 storms per year and the advisories  
595 72, hence the advisories have  $\sim 4\%$  more storms, whereas for the SH, IBTrACS has on average 28  
596 storms per year and the advisories 39, hence the advisories have  $\sim 40\%$  more storms. Hence in the  
597 NH it appears that a much larger proportion of the storms in the advisories make their way into  
598 the best track data than in the SH. This can partially explain the difference in numbers between  
599 IBTrACS and the TCs identified by the objective detection method in the reanalyses in the SH. It  
600 was discussed in the Matching Against IBTrACS subsection that some of the storms identified in  
601 the reanalyses appeared to be in the advisories but not IBTrACS.

602 Tropical disturbances and subtropical cyclones occur in all the ocean basins, and it seems that  
603 whether or not they contribute to the best track data may vary between the NH and SH and be  
604 dependent on the warning center procedures. The SPCZ and South Atlantic Convergence Zone  
605 (SACZ) are known to be associated with weak tropical depressions and subtropical cyclones in the

606 SH, as well as more intense tropical cyclones in the South Pacific (Vincent et al. 2011). A similar  
607 situation occurs in the North Pacific associated with the Mei-Yu front (Lee et al. 2006). The South  
608 Atlantic is not known as a very active TC region, due to relatively cool Sea Surface Temperatures  
609 and relatively high vertical wind shear. However, several studies have highlighted this region as  
610 susceptible to the formation of subtropical cyclones (Evans and Braun 2012; Gozzo et al. 2014)  
611 often in association with the SACZ. This is also seen in simulations produced with high-resolution  
612 GCMs where they are often identified as TCs (Roberts et al. 2015). The study of Gozzo et al.  
613 (2014), based on reanalysis data, found on average 7 subtropical cyclones per year with genesis  
614 between 20-30<sup>0</sup>S, a number that is remarkably similar to the number of systems objectively de-  
615 tected in the reanalyses in this study in the SA region. The majority of the sub-tropical cyclones  
616 identified by Gozzo et al. (2014) do not seem to have made it into the advisories or best track data,  
617 either because they are too weak, even for the advisories, or possibly because in general they are  
618 moving away from land and therefore not a threat (Kucas et al. 2014). Another possibility is that  
619 SA sub-tropical cyclones are more asymmetric than those found in the North Atlantic (Evans and  
620 Braun 2012) and hence do not satisfy the criteria for inclusion in the TC best tracks. A similar  
621 situation may also occur in the South Pacific. If these additional uncertainties in the best track data  
622 are considered together with the numbers in the advisory data, then the actual numbers of TCs  
623 occurring in the SH may not be too far away from the numbers objectively identified here in the  
624 reanalyses. The results from the Matching Against IBTrACS subsection suggest that some of the  
625 differences between numbers in the SH between the objective identification used in this study and  
626 IBTrACS may be related to the identification of hybrid or sub-tropical cyclones by the objective  
627 identification scheme.

628 Other regions where subtropical or hybrid storms may need to be considered are the cool seasons  
629 in the eastern north Pacific, where they are called Kona storms (Kodama and Businger 1998).

630 Monsoon depressions may also be confused with weak tropical cyclones in the reanalyses as these  
631 also have a warm core aloft structure and occur in the north and south Indian ocean, western  
632 Pacific and Australian region (Hurley and Boos 2015). They represent an additional uncertainty  
633 in the best track archive, as they are occasionally included in the best track data in the western  
634 Pacific via the JTWC (Hurley and Boos 2015); however, as with subtropical cyclones, this is not  
635 done consistently for all agencies. These may also contribute to uncertainties in the best track data  
636 in the north and south Indian ocean and South Pacific.

637 The second possibility for the differences in the numbers of TCs detected by the objective detec-  
638 tion method in the reanalyses and IBTrACS in the NH and SH concerns the quality of the reanaly-  
639 ses in the two hemispheres, which may affect how TCs are represented and hence contribute to the  
640 uncertainties in their detection in the reanalyses. The primary observations assimilated in the SH  
641 come from satellite observing platforms, which generally provide relatively coarse vertical reso-  
642 lutions, whereas in the NH the surface-based observing system provides a more diverse range of  
643 observations, including from sondes and aircraft. The use of direct satellite radiance assimilation,  
644 variational bias correction and modern assimilation methods has resulted in much better extraction  
645 of the information content in the observations, including for older observations (Rienecker et al.  
646 2012). Discriminating between weak TSs, sub-tropical cyclones and other systems in the reanal-  
647 yses is a problem in both hemispheres for the objective detection method, but could be more of  
648 a problem in the SH if the TCs are not as well simulated and storms, including sub-tropical or  
649 hybrid storms, do not have the correct structure. This could be exacerbated if there are more of  
650 the weaker type of storms in the SH associated with the convergence zones as discussed above,  
651 which, allied to the difficulty in separating these storms from other systems, may be a factor in  
652 the differences between the number of storms in IBTrACS and the number detected by the objec-  
653 tive detection method in the reanalyses in the SH. The only way to test this is by using observing

654 system experiments, where the NH observing system is degraded to that of the SH and the data as-  
655 simulation re-run. These types of experiments have been performed in the past and have shown the  
656 relative importance of the different types of observations used in the reanalyses and how changes  
657 to the observing system may affect the reanalysis (Bengtsson et al. 2004b; Whitaker et al. 2009).  
658 However, it is very time consuming and expensive to re-run modern data assimilation systems,  
659 even if we had access to the same systems used to produce the reanalyses used here. Hence this is  
660 beyond the scope of this paper. However, studies using the same detection criteria as used here,  
661 applied to relatively high resolution climate model simulations for the current climate (Gleixner  
662 et al. 2013; Strachan et al. 2013; Roberts et al. 2015), have found similar results to those found  
663 here for the reanalyses, in that similar TC numbers to observations are found in the NH, albeit with  
664 some model dependent basin by basin biases, and a larger number of TCs than in the observations  
665 in the SH. This may indicate that the difference in the number of SH storms from the observations  
666 are not necessarily related to differences in the quality of the reanalyses in the two hemispheres,  
667 but more with possible biases in the best track data and possibly the detection criteria used in our  
668 objective scheme, discussed next.

669 The larger bias in the number of TCs identified by the objective detection method in the SH  
670 compared with the NH relative to observations may also be related to the detection criteria used  
671 here, and whether they are selective enough for the data used, so that more tropical depressions,  
672 subtropical cyclones and hybrid cyclones are identified as TCs, possibly related to the quality of  
673 the reanalyses as discussed above. TC detection schemes, applied to model or reanalysis data,  
674 are certainly sensitive to the detection criteria and tracking methodology employed (Horn et al.  
675 2014), especially for weaker storms, as shown in this paper, and are most often tuned for the  
676 NH. An alternative approach would be to apply more selective criteria to remove subtropical and  
677 hybrid cyclones from the detection, based on previous studies focussed on studying subtropical

678 cyclones, for example the Hart phase space parameters (Guishard et al. 2009; Evans and Braun  
679 2012; Yanase et al. 2014). Another idea in the literature suggests using TC development pathways  
680 (McTaggart-Cowan et al. 2013), whereby tropical cyclogenesis is categorized according to dy-  
681 namical metrics, although this would necessarily introduce added complexity and possibly more  
682 parameters to choose subjectively. It would also remove these types of storms in the NH, so that,  
683 whilst the numbers detected in the SH may compare better with the observations, the numbers may  
684 compare less favourably in the NH. However, it might allow a better focus on the different storm  
685 types.

686 It is likely that all three of the issues discussed above can lead to TC detection biases in the  
687 reanalyses relative to the best track data.

688 No TC tracking and/or identification scheme will be perfect and, although TC identification  
689 schemes can be re-tuned against the observations separately for the NH and SH or for individual  
690 ocean basins if necessary (Camargo and Zebiak 2002) to take account of possible deficiencies in  
691 the detection and the observational biases, this does not seem like a good idea if TC detection is  
692 to be applied to model simulations where methodological consistency is important.

## 693 **5. Summary and conclusions**

694 The study of TCs in six recent reanalyses has shown that all the reanalyses are capable of rep-  
695 resenting nearly all the TCs present in the best track archive of IBTrACS, with a detection rate of  
696  $\sim 98\%$  in the period since 2000 and slightly lower before this. However, how well the TCs are  
697 represented in the reanalyses, in terms of their properties, is less encouraging, with wind intensities  
698 significantly lower than in the observations and pressures too high in value. Although significant  
699 amounts of observations are assimilated by the data assimilation systems used in the reanalyses,  
700 in particular from satellites, this is unable to correct these deficiencies in the TC properties, due

701 to the still too low model resolution and dependence on parameterized processes used in the re-  
702 analyses. Additional methods of assimilating observations in the vicinity of the TCs and vortex  
703 relocation can help improve this situation, but not to the extent where intensities get anywhere near  
704 those observed at current reanalysis resolutions. However, it is apparent that there has been some  
705 improvements in the representation of TCs in the more recent reanalyses of NCEP-CFSR, JRA55  
706 and MERRA2; in particular MERRA2 shows a significant improvement over the older MERRA  
707 reanalysis in terms of wind and MSLP intensities. Separation distances between TCs identified  
708 in the reanalyses and the observations have also improved with the more recent reanalyses. The  
709 improvements in the intensities and location are most likely due to the increases in model horizon-  
710 tal resolutions and the use of improved data assimilation and bias correction systems, which are  
711 capable of extracting more information content from the older observations, as well as resulting in  
712 less observation rejection and the introduction of new and better calibrated observing systems in  
713 recent years. This progress is likely to continue as new reanalyses are produced with ever higher  
714 resolutions, such as the new ECMWF ERA5 reanalysis. Further improvements in data assimilation  
715 are expected as well as the introduction of new and more accurate observing systems, although the  
716 downside to this may be the introduction of spurious trends in TC properties.

717 The other aspect explored in this study is how well objective TC detection schemes are capable  
718 of detecting the same TCs that are in the observations using a widely used identification scheme.  
719 This is important in order to have confidence in these schemes when applied to climate model sim-  
720 ulations and for comparisons made between models or experiment scenarios. This part of the study  
721 highlighted the problem of detecting TCs at the low intensity end of the TC intensity range: in par-  
722 ticular, tropical depressions and up to category 1 (Saffir-Simpson), with gradual improvements in  
723 the detection rate with increasing TS category. This raises several issues: are the current detection  
724 schemes used at operational centers and for climate studies of TCs, which all have a rather similar

725 methodology of user chosen thresholds on intensity and/or structure, selective enough; are TCs  
726 represented well enough in the reanalyses; are there problems with observational biases for weak  
727 storms? The answer to these questions is probably that all three play a role in differences found  
728 between the objective identification of TCs in reanalyses and the observed best track data. It is  
729 clear the intensities, and probably structure, are not well enough simulated in the reanalyses, which  
730 will cause problems when trying to discriminate between weak TSs and other tropical systems. In  
731 terms of more selective criteria, other approaches could certainly be introduced, such as the phase  
732 space approach, but this will also depend on how well TCs are represented in the reanalyses and  
733 the introduction of subjective thresholds on the phase space parameters (Yanase et al. 2014). How-  
734 ever, it may be useful in removing the need for artificial boundaries in the TC identification such  
735 as the latitude band for genesis used in this study. The problem of observational bias is also an im-  
736 portant aspect, in particular for the weaker storms, since forecaster interpretation and subjectivity  
737 will play a role in whether a particular storm is included in the best track data, as not all storms fall  
738 neatly into particular classifications. Allied to this are the different operational criteria employed  
739 by the different RSMC, which contribute data to the best track archives, such as whether to include  
740 tropical depressions or subtropical cyclones. This is likely the primary cause of the differences be-  
741 tween the number of TCs identified in the reanalyses and IBTrACS, in particular in the SH. This  
742 makes the observations less than ideal for calibrating TC identification and tracking schemes, or  
743 indeed in their use in global climatological studies of TC frequencies and variability. It could be  
744 concluded that, given the uncertainties in the best track data sets, they should not be considered  
745 climate quality data sets. Better coordination between the RSMCs would help this situation go-  
746 ing forward, although this is not necessarily part of their remit and their operational procedures  
747 are tailored to their region of responsibility. The problems of objectively classifying TCs opera-  
748 tionally has been recognized by the Seventh International Workshop on Tropical Cyclones who

749 have suggested that "a substantial contribution to the operational TC forecasting community could  
750 be made by recommending a universal cyclone classification methodology based on the latest re-  
751 search, operational forecasting capabilities, and real-time data availability". A re-evaluation of the  
752 observational record over the satellite period using a combination of the satellite data and reanaly-  
753 ses, using consistent identification methods for all basins, could perhaps resolve the observational  
754 bias problem over historical periods covered by the satellites and provide a more complete record  
755 of tropical storms for use in risk assessment and validating climate models. There has been some  
756 discussion that tropical depressions and subtropical cyclones should be included in the best track  
757 data for consistency (McAdie et al. 2009), since, before satellite observations became available,  
758 some subtropical systems were probably classified as TSs. Tropical depressions and subtropical  
759 cyclones are also associated with severe weather with TS like properties of strong winds and pre-  
760 cipitation (Guishard et al. 2009; Gyakum 2011), so their inclusion can be justified in terms of their  
761 impact and for a more complete record of TC activity.

762 Whilst there are deficiencies in the representation of TCs in the reanalyses, and 10 m winds in  
763 particular should be used with caution, they can be complementary to the observations and provide  
764 added value information on TCs such as the pre- and post-TC stages of the lifecycle. For example,  
765 the tracking method used here identifies these earlier and later lifecycle stages, which can then be  
766 used to study the early development of TCs and their environment and the extratropical transition  
767 (Studholme et al. 2015) and how storms behave after this. The extratropical transition and its  
768 aftermath are becoming increasingly important for risk analysis at high latitudes following cases  
769 such as hurricane Sandy and Gonzalo and recent studies such as Haarsma et al. (2013) and is a  
770 known contributor to forecast uncertainty in the extra-tropics (Anwender and Harr 2008).

771 *Acknowledgments.* The authors would like to thank the various data archive centers for making  
772 the data used in this study available. ERA-Interim data provided courtesy ECMWF. MERRA was  
773 developed by the Global Modeling and Assimilation Office and supported by the NASA Model-  
774 ing, Analysis and Prediction Program. Source data files can be acquired from the Goddard Earth  
775 Science Data Information Services Center (GES DISC). The NCEP-CFSR data set used for this  
776 study is provided from the Climate Forecast System Reanalysis (CFSR) project carried out by the  
777 Environmental Modeling Center (EMC), National Centers for Environmental Prediction (NCEP).  
778 The JRA25 data set used for this study is provided from the Japanese 25-year Reanalysis (JRA-  
779 25), a cooperative research project carried out by the Japan Meteorological Agency (JMA) and  
780 the Central Research Institute of Electric Power Industry (CRIEPI). The JRA55 data set used for  
781 this study is provided from the Japanese 55-year Reanalysis (JRA-55) project carried out by the  
782 Japan Meteorological Agency (JMA). Vidale acknowledges funding from the Willis Chair in Cli-  
783 mate System Science and Climate Hazards. Cobb acknowledges funding from the “Innovate UK”  
784 Knowledge Transfer Partnership (KTP). The authors would also like to thank the two reviewers  
785 for their constructive comments leading to an improved paper.

## 786 **References**

- 787 Adeola, F. O., and J. S. Picou, 2014: Social capital and the mental health impacts of hurricane  
788 katrina: assessing long-term patterns of psychosocial distress. *International Journal of Mass  
789 Emergencies and Disasters*, **32** (1), 121–156.
- 790 Anwender, D., and S. C. Harr, P. A .and Jones, 2008: Predictability associated with the down-  
791 stream impacts of the extratropical transition of tropical cyclones: Case studies. *Mon. Wea. Rev.*,  
792 **136**, 3226–3247.

- 793 Barcikowska, M., F. Feser, and H. Von Storch, 2012: Usability of best track data in climate statis-  
794 tics in the western north pacific. *Monthly Weather Review*, **140** (9), 2818–2830.
- 795 Bell, R., J. Strachan, P. L. Vidale, K. I. Hodges, and M. Roberts, 2013: Response of tropical  
796 cyclones to idealized climate change experiments in a global high-resolution coupled general  
797 circulation model. *J. Clim.*, **26**, 7966–7980.
- 798 Bengtsson, L., M. Botzet, and M. Esch, 1995: Hurricane-type vortices in a general circulation  
799 model. *Tellus*, **47A**, 175196.
- 800 Bengtsson, L., S. Hagemann, and K. I. Hodges, 2004a: Can climate trends be calculated  
801 from reanalysis data? *Jgr-atmos.*, *J. Geophys. Res. Atmos.*, **109**, doi:D11111,doi:10.1029/  
802 2004JD004536.
- 803 Bengtsson, L., K. Hodges, and M. Esch, 2007a: Tropical cyclones in a t159 resolution global  
804 climate model: Comparison with observations and re-analyses. *Tellus A*, **59** (4), 396–416.
- 805 Bengtsson, L., K. I. Hodges, M. Esch, N. Keenlyside, L. Kornbluh, J.-J. Luo, and T. Yamagata,  
806 2007b: How may tropical cyclones change in a warmer climate? *Tellus*, **59A**, 539–561.
- 807 Bengtsson, L., K. I. Hodges, and S. Hagemann, 2004b: Sensitivity of the era40 reanalysis to the  
808 observing system: determination of the global atmospheric circulation from reduced observa-  
809 tions. *Tellus*, **56A**, 456–471.
- 810 Bentley, A., M. D. Keyser, and L. F. Bosart, 2016: A dynamically based climatology of subtropical  
811 cyclones that undergo tropical transition in the north atlantic basin. *Mon. Wea. Rev.*, **144**, 2049–  
812 2068.
- 813 Bloom, S. C., L. L. Takacs, A. M. da Silva, and D. Ledvina, 1996: Data assimilation using incre-  
814 mental analysis updates. *Mon. Wea. Rev.*, **124**, 12561271.

815 Bosilovich, M. G., and coauthors, 2015: Merra-2: Initial evaluation of the climate. Techni-  
816 cal Report Series on Global Modeling and Data Assimilation, Volume 43 NASA/TM2015-  
817 104606/Vol. 43, National Aeronautics and Space Administration, Goddard Space Flight Center,  
818 Greenbelt, Maryland 20771, USA.

819 Camargo, S. J., A. G. Barnston, , and S. E. Zebiak, 2005: A statistical assessment of tropical  
820 cyclone activity in atmospheric general circulation models. *Tellus*, **57A**, 589604.

821 Camargo, S. J., and . Zebiak, S. E. 17, 2002: Improving the detection and tracking of tropical  
822 storms in atmospheric general circulation models. *Wea. Forecasting*, **17**, 11521162.

823 Davis, C., and Coauthors, 2008: Prediction of landfalling hurricanes with the advanced hurricane  
824 wrf model. *Mon. Wea. Rev.*, **136**, 19902005.

825 Dee, D., and Coauthors, 2011: The era-interim reanalysis: Configuration and performance of the  
826 data assimilation system. *Quarterly Journal of the Royal Meteorological Society*, **137 (656)**,  
827 553–597.

828 Dee, D. P., and S. M. Uppala, 2009: Variational bias correction of satellite radiance data in the  
829 era-interim reanalysis. *Q. J. R. Meteorol. Soc.*, **135**, 18301841.

830 Diamond, H., A. M. Lorrey, K. R. Knapp, and D. H. Levinson, 2012: Development of an enhanced  
831 tropical cyclone tracks database for the southwest pacific from 1840-2010. *Int. J. Climatol.*, **32**,  
832 22402250.

833 ECMWF, 2015: *Part IV: Physical Processes*. IFS Documentation, ECMWF, operational imple-  
834 mentation 12 May 2015.

835 Evans, J. L., and A. Braun, 2012: A climatology of subtropical cyclones in the south atlantic. *J*  
836 *Climate*, **25**, 73287340.

837 Fine, C. M., R. H. Johnson, P. E. Ciesielski, and R. K. Taft, 2016: The role of topographically  
838 induced vortices in tropical cyclone formation over the indian ocean. *Mon. Wea. Rev.*, **144**, 4827–  
839 4847.

840 for the Caribbean, S. H., 2009: Belize: Macro socio-economic assessment of the damage and  
841 losses caused by tropical depression 16. Tech. rep., United Nations Economic Commission for  
842 Latin America and the Caribbean.

843 Gleixner, S., N. Keenlyside, K. I. Hodges, W.-L. Tseng, and L. Bengtsson, 2013: An inter-  
844 hemispheric comparison of the tropical storm response to global warming. *Climate Dynam-*  
845 *ics*, **42 (7-8)**, 2147–2157, doi:10.1007/s00382-013-1914-6, URL [http://dx.doi.org/10.1007/](http://dx.doi.org/10.1007/s00382-013-1914-6)  
846 [s00382-013-1914-6](http://dx.doi.org/10.1007/s00382-013-1914-6).

847 Gozzo, L. F., R. P. da Rocha, M. S. Reboita, and S. Sugahara, 2014: Subtropical cyclones over the  
848 southwestern south atlantic: Climatological aspects and case study. *J. Climate*, **27**, 85438562.

849 Guishard, M. P., J. L. Evans, and R. E. Hart, 2009: Atlantic subtropical storms. part ii: Climatol-  
850 ogy. *J. Climate*, **22**, 35743594.

851 Gyakum, J. R., 2011: Subtropical and hybrid systems. *Proc. Seventh Int. Workshop on Tropi-*  
852 *cal Cyclones*, Saint-Gilles-Les-Bains, La Runion, France, World Meteorological Organization,  
853 1.6.1-1.6.28, WMO/TD-1561.

854 Haarsma, R. J., W. Hazeleger, C. Severijns, H. de Vries, A. Sterl, R. Bintanja, G. J. van Olden-  
855 borgh, and H. W. van den Brink, 2013: More hurricanes to hit western europe due to global  
856 warming. *Geophys. Res. Lett.*, **40**, 17831788.

- 857 Harper, B., J. Kepert, and J. Ginger, 2010: Guidelines for converting between various wind av-  
858 eraging periods in tropical cyclone conditions. *World Meteorological Organization, WMO/TD*,  
859 **1555**.
- 860 Hart, R. E., 2003: A cyclone phase space derived from thermal wind and thermal asymmetry.  
861 *Monthly Weather Review*, **131 (4)**, 585–616.
- 862 Hatsushika, H., J. Tsutsui, M. Fiorino, and K. Onogi, 2006: Impact of wind profile retrievals on  
863 the analysis of tropical cyclones in the jra-25 reanalysis. *J. 2*, **84 (5)**, 891–905.
- 864 Hodges, K. I., 1994: A general-method for tracking analysis and its application to meteorological  
865 data. *Monthly Weather Review*, **122 (11)**, 2573–2586.
- 866 Hodges, K. I., 1995: Feature tracking on the unit sphere. *Monthly Weather Review*, **123 (12)**,  
867 3458–3465.
- 868 Hodges, K. I., 1999: Adaptive constraints for feature tracking. *Monthly Weather Review*, **127 (6)**,  
869 1362–1373.
- 870 Hodges, K. I., and R. Emerton, 2015: The prediction of northern hemisphere tropical cyclone ex-  
871 tended life cycles by the ecmwf ensemble and deterministic prediction systems. part i: Tropical  
872 cyclone stage. *Monthly Weather Review*, **143**, 50915114, doi:10.1175/MWR-D-13-00385.1.
- 873 Hodges, K. I., B. J. Hoskins, J. Boyle, and C. Thorncroft, 2003: A comparison of recent reanalysis  
874 datasets using objective feature tracking: Storm tracks and tropical easterly waves. *Monthly*  
875 *Weather Review*, **131 (9)**, 2012–2037.
- 876 Horn, M., and Coauthors, 2014: Tracking scheme dependence of simulated tropical cyclone re-  
877 sponse to idealized climate simulations. *Journal of Climate*, **27 (24)**, 9197–9213.

- 878 Hurley, J. V., and W. R. Boos, 2015: A global climatology of monsoon low-pressure systems.  
879 *Q.J.R. Meteorol. Soc.*, **141**, 10491064.
- 880 Jones, S. C., and Coauthors, 2003: The extratropical transition of tropical cyclones: Forecast  
881 challenges, current understanding, and future directions. *Weather and Forecasting*, **18**, 1052–  
882 1092.
- 883 Kilic, C., and C. C. Raible, 2013: Investigating the sensitivity of hurricane intensity and trajec-  
884 tory to sea surface temperatures using the regional model wrf. *Meteorologische Zeitschrift*, **22**,  
885 685698.
- 886 Kimball, S. K., and M. S. Mulekar, 2004: A 15-year climatology of north atlantic tropical cy-  
887 clones. part i: Size parameters. *J. Clim.*, **17**, 3555–3575.
- 888 King, R. O., 2013: Financing natural catastrophe exposure: Issues and options for improving risk  
889 transfer markets. ...., Congressional Research Service, Library of Congress.
- 890 Knaff, J. A., and R. M. Zehr, 2007: Reexamination of tropical cyclone windpressure relationships.  
891 *Wea. Forecasting*, **22**, 7188.
- 892 Knapp, K. R., M. C. Kruk, D. H. Levinson, H. J. Diamond, and C. J. Neumann, 2010: The  
893 international best track archive for climate stewardship (ibtracs) unifying tropical cyclone data.  
894 *Bulletin of the American Meteorological Society*, **91** (3), 363–376.
- 895 Kobayashi, S., and Coauthors, 2015: The jra-55 reanalysis: General specifications and basic char-  
896 acteristics. *J. Met. Soc. Jap.*, **93**, 5–48, doi:10.1175/JCLI-D-14-00005.1.
- 897 Kodama, K., and S. Businger, 1998: Weather and forecasting challenges in the pacific region of  
898 the national weather service. *Wea. Forecasting*, **13**, 253276.

- 899 Kucas, M., S. J. Barlow, and R. C. Ballucanag, 2014: Subtropical cyclones: Operational practices  
900 and analysis methods applied at the joint typhoon warning center. *Extended abstracts, 31st*  
901 *Conference on Hurricanes and Tropical Meteorology*, San Diego, CA, Amer. Meteor. Soc., 1-8.
- 902 Kueh, M.-T., 2012: Multiformality of the tropical cyclone windpressure relationship in the western  
903 north pacific: discrepancies among four best-track archives. *Environ. Res. Lett.*, **7**, doi:10.1088/  
904 1748-9326/7/2/024015.
- 905 Landsea, C., 2007: Counting atlantic tropical cyclones back to 1900. *Eos, Transactions American*  
906 *Geophysical Union*, **88 (18)**, 197–202.
- 907 Landsea, C. W., and J. L. Franklin, 2013: Atlantic hurricane database uncertainty and presentation  
908 of a new database format. *Monthly Weather Review*, **141 (10)**, 3576–3592.
- 909 Landsea, C. W., G. A. Vecchi, L. Bengtsson, and T. R. Knutson, 2009: Impact of duration thresh-  
910 olds on atlantic tropical cyclone counts. *J. Climate*, **23**, 25082519, doi:10.1175/2009JCLI3034.  
911 1.
- 912 Lee, C.-S., Y.-L. Lin, and K. K. Cheung, 2006: Tropical cyclone formations in the south china sea  
913 associated with the mei-yu front. *Mon. Wea. Rev.*, **134**, 26702687.
- 914 Manganello, J., and Coauthors, 2012: Tropical cyclone climatology in a 10-km global atmospheric  
915 gcm: Toward weather-resolving climate modeling. *J. Clim.*, **25,3867-3893.**, 3867–3893.
- 916 McAdie, C. J., C. W. Landsea, C. J. Neumann, J. E. David, E. S. Blake, and G. R. Hammer,  
917 2009: *Tropical cyclones of the north atlantic ocean, 1851 2006*. pp237, National Climatic Data  
918 Center, Asheville, NC, in cooperation with the National Hurricane Center, Miami, FL.

919 McTaggart-Cowan, R., T. J. Galarneau, L. F. Bosart, R. W. Moore, and O. Martius, 2013: A  
920 global climatology of baroclinically influenced tropical cyclogenesis. *Mon. Wea. Rev.*, **141**,  
921 1963–1989.

922 Molod, A., L. Takacs, M. Suarez, and J. Bacmeister, 2015: Development of the geos-5 atmospheric  
923 general circulation model: evolution from merra to merra2. *Geosci. Model Dev.*, **8**, 13391356.

924 Murakami, H., 2014: Tropical cyclones in reanalysis data sets. *Geophysical Research Letters*,  
925 **41 (6)**, 2133–2141.

926 Onogi, K., and Coauthors, 2007: The jra-25 reanalysis. *J. Met. Soc. Jap*, **85**, 369–432, doi:10.  
927 2151/jmsj.85.369.

928 Padgett, G., and S. Young, 2016: Global tropical cyclones summaries and operational track  
929 data. URL [https://australiasevereweather.com/cyclones/tropical\\_cyclone\\_summaries\\_track\\_data.](https://australiasevereweather.com/cyclones/tropical_cyclone_summaries_track_data.htm)  
930 [htm](https://australiasevereweather.com/cyclones/tropical_cyclone_summaries_track_data.htm), Accessed 13/10/2016.

931 Ren, F., J. Liang, G. Wu, W. Dong, and X. Yang, 2011: Reliability analysis of climate change of  
932 tropical cyclone activity over the western north pacific. *J Climate*, **24**, 58875898.

933 Rienecker, M. M., and Coauthors, 2012: Atmospheric reanalyses recent progress and prospects  
934 for the future. a report from a technical workshop, april 2010. NASA Technical Report Series  
935 on Global Modeling and Data Assimilation, 29 NASA TM2012-104606.

936 Rienecker, M. R., and coauthors, 2011: Merra - nasa's modern-era retrospective analysis for re-  
937 search and applications. *J. Climate*, **24**, 3624–3648, doi:10.1175/JCLI-D-11-00015.1.

938 Roberts, M. J., and Coauthors, 2015: Tropical cyclones in the upscale ensemble of high-resolution  
939 global climate models\*. *Journal of Climate*, **28 (2)**, 574–596.

940 Roth, D. M., 2002: A fifty year history of subtropical cyclones. *Preprints, 25th Conf. on Hur-*  
941 *ricanes and Tropical Meteorology, San Diego, CA, Amer. Meteor. Soc.*, P1.43, URL [http:](http://ams.confex.com/ams/pdfpapers/37402.pdf)  
942 [//ams.confex.com/ams/pdfpapers/37402.pdf](http://ams.confex.com/ams/pdfpapers/37402.pdf).

943 Sardeshmukh, P. D., and B. J. Hoskins, 1984: Spectral smoothing on the sphere. *Mon. Wea. Rev.*,  
944 **112**, 2524–2529.

945 Schenkel, B. A., and R. E. Hart, 2012: An examination of tropical cyclone position, intensity, and  
946 intensity life cycle within atmospheric reanalysis datasets. *J. Climate*, **25**, 3453–3475.

947 Schreck III, C. J., K. R. Knapp, and J. P. Kossin, 2014: The impact of best track discrepancies on  
948 global tropical cyclone climatologies using ibtracs. *Monthly Weather Review*, **142** (10), 3881–  
949 3899.

950 Serra, Y. L., G. N. Kiladis, and K. I. Hodges, 2010: Tracking and mean structure of easterly waves  
951 over the intra-americas sea. *Journal of Climate*, **23** (18), 4823–4840.

952 Shaevitz, D. A., and Coauthors, 2014: Characteristics of tropical cyclones in high-resolution mod-  
953 els in the present climate. *J. Adv. Model. Earth Syst.*, **6**, 11541–1172., 11541–1172.,

954 Shao, H., and Coauthors, 2016: Bridging research to operations transitions: Status and plans of  
955 community gsi. *Bulletin of the American Meteorological Society*, **97**, 1427–1440.

956 Strachan, J., P. L. Vidale, K. Hodges, M. Roberts, and M.-E. Demory, 2013: Investigating global  
957 tropical cyclone activity with a hierarchy of agcms: The role of model resolution. *Journal of*  
958 *Climate*, **26** (1), 133–152.

959 Studholme, J., K. I. K. I. Hodges, and C. M. Brierley, 2015: Objective determination of the ex-  
960 tratropical transition of tropical cyclones in the northern hemisphere. *Tellus*, **67A**, 24–474, URL  
961 <http://dx.doi.org/10.3402/tellusa.v67.24474>.

- 962 Suranjana, S., and Coauthors, 2010: The ncep climate forecast system reanalysis. *Bulletin of the*  
963 *American Meteorological Society*, **91**, 1015–1057.
- 964 Torn, R. D., and C. Snyder, 2012: Uncertainty of tropical cyclone best-track information. *Weather*  
965 *and Forecasting*, **27** (3), 715–729.
- 966 Truchelut, R., R. Hart, and B. Luthman, 2013: Global identification of previously undetected  
967 pre-satellite era tropical cyclone candidates in noaa/cires 20th century reanalysis data. *J. Appl.*  
968 *Meteor. Climatol.*, **52**, 2243–2259, doi:10.1175/JAMC-D-12-0276.1.
- 969 Velden, C., and Coauthors, 2006a: The dvorak tropical cyclone intensity estimation technique: A  
970 satellite-based method that has endured for over 30 years. *Bulletin of the American Meteorolog-*  
971 *ical Society*, **87**, 1195–1210.
- 972 Velden, C., and Coauthors, 2006b: Supplement to: The dvorak tropical cyclone intensity estima-  
973 tion technique: A satellite-based method that has endured for over 30 years. *Bull.Amer.Met.Soc.*,  
974 **87**, S6–S9.
- 975 Vincent, E. M., M. Lengaigne, C. E. Menkes, N. C. Jourdain, P. Marchesiello, and . Madec,  
976 2011: Interannual variability of the south pacific convergence zone and implications for tropical  
977 cyclone genesis. *Climate Dynamics*, **36**, 1881–1896.
- 978 Walsh, K. J. E., M. Fiorino, C. W. Landsea, and K. L. McInnes, 2007: Objectively determined  
979 resolution-dependent threshold criteria for the detection of tropical cyclones in climate models  
980 and reanalyses. *J. Clim.*, **20**, 23072314.
- 981 Whitaker, J. S., G. P. Compo, and J.-N. Thpaut, 2009: A comparison of variational and ensemble-  
982 based data assimilation systems for reanalysis of sparse observations. *Mon. Weather Rev.*, **137**,  
983 19911999.

984 Wu, C.-C., and Coauthors, 2005: Dropwindsonde observations for typhoon surveillance near the  
985 taiwan region (dotstar). *Bull. Amer. Met. Soc.*, **86**, 787–790.

986 Yanase, W., H. Niino, K. I. Hodges, and N. Kitabatake, 2014: Parameter spaces of environmental  
987 fields responsible for cyclone development from tropics to extratropics. *J. Climate*, **27**, 652671.

988 **LIST OF TABLES**

989 **Table 1.** Summary of the reanalysis datasets used in this study. Abbreviations, 4D-Var,  
990 4D variational assimilation ; 3D-Var, 3D variational assimilation; TL255L60,  
991 triangular truncation 255, linear grid, 60 vertical levels; GSI, Grid-point statisti-  
992 cal interpolation; IAU, Incremental Analysis Update. . . . . 47

993 **Table 2.** The POD for the NH and SH for the direct matching method applied to the  
994 reanalysis tracks (c.f. Direct Matching Results section) and the POD and FAR  
995 for the NH and SH based on the objective detection method (c.f. Matching  
996 Against IBTrACS subsection). . . . . 48

997 **Table 3.** Storms that match and don't match with IBTrACS in the NH by storm category,  
998 for storms identified by the objective detection method applied to the reanaly-  
999 sis tracks, in the first column for each reanalysis, and for the direct matching  
1000 method performed in the Direct Matching Results subsection in the second col-  
1001 umn with brackets for each reanalysis. Values are number per year. . . . . 49

1002 **Table 4.** Same as Table 2 but for the SH. . . . . 50

1003 **Table 5.** The POD for the NH and SH for the TC obtained from the reanalyses by the  
1004 objective detection method that match with the observed Cat1-Cat5 TS only. . . . . 51

1005 TABLE 1. Summary of the reanalysis datasets used in this study. Abbreviations, 4D-Var, 4D variational  
 1006 assimilation ; 3D-Var, 3D variational assimilation; TL255L60, triangular truncation 255, linear grid, 60 vertical  
 1007 levels; GSI, Grid-point statistical interpolation; IAU, Incremental Analysis Update.

	<i>ERA-Interim</i>	<i>JRA25</i>	<i>JRA55</i>	<i>NCEP-CFSR</i>	<i>MERRA</i>	<i>MERRA2</i>
Assimilation	4D-Var	3D-Var	4D-Var	3D-Var	3D-VAR	3D-Var
				GSI	GSI+IAU	GSI+IAU
Model	TL255L60	T106L40	TL319L60	T382L64	$1/2^0 \times 2/3^0$ L72	Cubed Sphere
Resolution	(80km)	(120km)	(55km)	(38km)	(55km)	(50km)
Data Grid	$512 \times 256$	$288 \times 145$	$288 \times 145$	$720 \times 361$	$540 \times 361$	$576 \times 361$

1008 TABLE 2. The POD for the NH and SH for the direct matching method applied to the reanalysis tracks (c.f.  
 1009 Direct Matching Results section) and the POD and FAR for the NH and SH based on the objective detection  
 1010 method (c.f. Matching Against IBTrACS subsection).

POD						
	<i>ERA-Interim</i>	<i>JRA25</i>	<i>JRA55</i>	<i>NCEP-CFSR</i>	<i>MERRA</i>	<i>MERRA2</i>
NH Direct Match	0.95	0.95	0.95	0.95	0.95	0.95
NH Objective	0.60	0.76	0.80	0.70	0.51	0.67
SH Direct Match	0.93	0.93	0.94	0.93	0.90	0.93
SH Objective	0.76	0.84	0.87	0.83	0.61	0.79
FAR						
NH Objective	0.28	0.16	0.29	0.36	0.21	0.36
SH Objective	0.60	0.43	0.58	0.58	0.54	0.63

1011 TABLE 3. Storms that match and don't match with IBTrACS in the NH by storm category, for storms identified  
 1012 by the objective detection method applied to the reanalysis tracks, in the first column for each reanalysis, and  
 1013 for the direct matching method performed in the Direct Matching Results subsection in the second column with  
 1014 brackets for each reanalysis. Values are number per year.

Category		<i>ERA-Interim</i>	<i>JRA25</i>	<i>JRA55</i>	<i>NCEP-CFSR</i>	<i>MERRA</i>	<i>MERRA2</i>
TD	Match	2.91 ( 7.94)	3.26 ( 7.94)	5.24 ( 8.03)	3.50 ( 8.00)	2.29 ( 7.85)	3.48 ( 7.67)
	No Match	5.56 ( 0.53)	5.21 ( 0.53)	3.24 ( 0.44)	4.97 ( 0.47)	6.18 ( 0.62)	4.91 ( 0.73)
TS	Match	11.85 (22.38)	18.62 (22.53)	18.32 (22.53)	14.76 (22.32)	9.85 (22.44)	14.24 (22.45)
	No Match	11.85 ( 1.32)	5.09 ( 1.18)	5.38 ( 1.18)	8.94 ( 1.38)	13.85 ( 1.26)	9.73 ( 1.52)
CAT1	Match	8.74 (12.23)	11.18 (12.23)	11.17 (12.24)	10.09 (12.12)	7.74 (12.21)	9.76 (12.33)
	No Match	3.44 ( 0.00)	1.00 ( 0.00)	1.00 ( 0.00)	2.09 ( 0.06)	4.44 ( 0.00)	2.55 ( 0.00)
CAT2	Match	5.29 ( 6.35)	6.15 ( 6.38)	6.00 ( 6.35)	5.82 ( 6.38)	4.76 ( 6.35)	5.64 ( 6.39)
	No Match	1.06 ( 0.00)	0.21 ( 0.00)	0.35 ( 0.00)	0.53 ( 0.00)	1.59 ( 0.00)	0.73 ( 0.00)
CAT3	Match	6.15 ( 7.00)	6.91 ( 7.06)	6.82 ( 7.03)	6.71 ( 7.06)	5.82 ( 7.03)	6.42 ( 7.06)
	No Match	0.88 ( 0.03)	0.12 ( 0.00)	0.21 ( 0.00)	0.32 ( 0.00)	1.21 ( 0.00)	0.64 ( 0.00)
CAT4	Match	5.97 ( 6.79)	6.76 ( 6.79)	6.71 ( 6.74)	6.47 ( 6.79)	5.76 ( 6.76)	6.48 ( 6.76)
	No Match	0.82 ( 0.00)	0.03 ( 0.00)	0.09 ( 0.06)	0.32 ( 0.00)	1.03 ( 0.03)	0.33 ( 0.06)
CAT5	Match	1.09 ( 1.12)	1.12 ( 1.12)	1.12 ( 1.12)	1.12 ( 1.12)	1.03 ( 1.12)	1.09 ( 1.09)
	No Match	0.03 ( 0.00)	0.00 ( 0.00)	0.00 ( 0.00)	0.00 ( 0.00)	0.09 ( 0.00)	0.00 ( 0.00)

TABLE 4. Same as Table 2 but for the SH.

Category		<i>ERA1</i>	<i>JRA25</i>	<i>JRA55</i>	<i>NCEP – CFSR</i>	<i>MERRA</i>	<i>MERRA2</i>
TD	Match	0.42 (0.58)	0.48 (0.61)	0.52 (0.58)	0.48 (0.61)	0.21 (0.49)	0.44 (0.48)
	No Match	0.18 (0.03)	0.12 (0.00)	0.09 (0.03)	0.12 (0.00)	0.39 (0.12)	0.13 (0.06)
TS	Match	7.15 (9.09)	8.03 (9.06)	8.55 (9.09)	7.76 (9.18)	5.67 (9.00)	7.59 (8.91)
	No Match	2.42 (0.48)	1.55 (0.51)	1.03 (0.48)	1.82 (0.39)	3.91 (0.58)	2.00 (0.39)
CAT1	Match	4.55 (5.36)	5.09 (5.36)	5.12 (5.39)	4.94 (5.39)	3.79 (5.33)	4.75 (5.21)
	No Match	0.88 (0.06)	0.33 (0.06)	0.30 (0.03)	0.48 (0.03)	1.64 (0.09)	0.69 (0.06)
CAT2	Match	2.21 (2.64)	2.58 (2.61)	2.55 (2.64)	2.52 (2.64)	2.03 (2.61)	2.38 (2.61)
	No Match	0.61 (0.18)	0.24 (0.21)	0.27 (0.18)	0.30 (0.18)	0.79 (0.21)	0.53 (0.21)
CAT3	Match	2.55 (2.73)	2.61 (2.70)	2.70 (2.73)	2.64 (2.70)	2.12 (2.70)	2.63 (2.73)
	No Match	0.18 (0.00)	0.12 (0.03)	0.03 (0.00)	0.09 (0.03)	0.61 (0.03)	0.19 (0.00)
CAT4	Match	2.69 (2.76)	2.73 (2.73)	2.64 (2.76)	2.76 (2.76)	2.33 (2.76)	2.78 (2.76)
	No Match	0.06 (0.00)	0.03 (0.03)	0.12 (0.00)	0.00 (0.00)	0.42 (0.00)	0.06 (0.00)
CAT5	Match	0.58 (0.58)	0.51 (0.52)	0.55 (0.58)	0.55 (0.55)	0.55 (0.58)	0.59 (0.58)
	No Match	0.00 (0.00)	0.06 (0.06)	0.03 (0.00)	0.03 (0.03)	0.03 (0.00)	0.00 (0.00)

1015 TABLE 5. The POD for the NH and SH for the TC obtained from the reanalyses by the objective detection  
 1016 method that match with the observed Cat1-Cat5 TS only.

	POD					
	<i>ERA1</i>	<i>JRA25</i>	<i>JRA55</i>	<i>NCEP-CFSR</i>	<i>MERRA</i>	<i>MERRA2</i>
NH Objective	0.81	0.96	0.95	0.90	0.75	0.87
SH Objective	0.88	0.91	0.95	0.94	0.75	0.92

1017 **LIST OF FIGURES**

1018 **Fig. 1.** Distribution of mean separation distances (geodesic degrees,  $1^0 \simeq 111km$ ) between the re-  
1019 analysis tracks and those of IBTrACS for tracks that match using the direct matching method  
1020 (c.f. Direct Matching Results subsection) (a) NH, (b) SH, distribution of lifetimes (days) for  
1021 the matched tracks (c) NH, (d) SH and the distribution of latitudes at which the matched  
1022 tracks attain the peak intensity based on the 10m winds (e) NH, (f) SH. . . . . 53

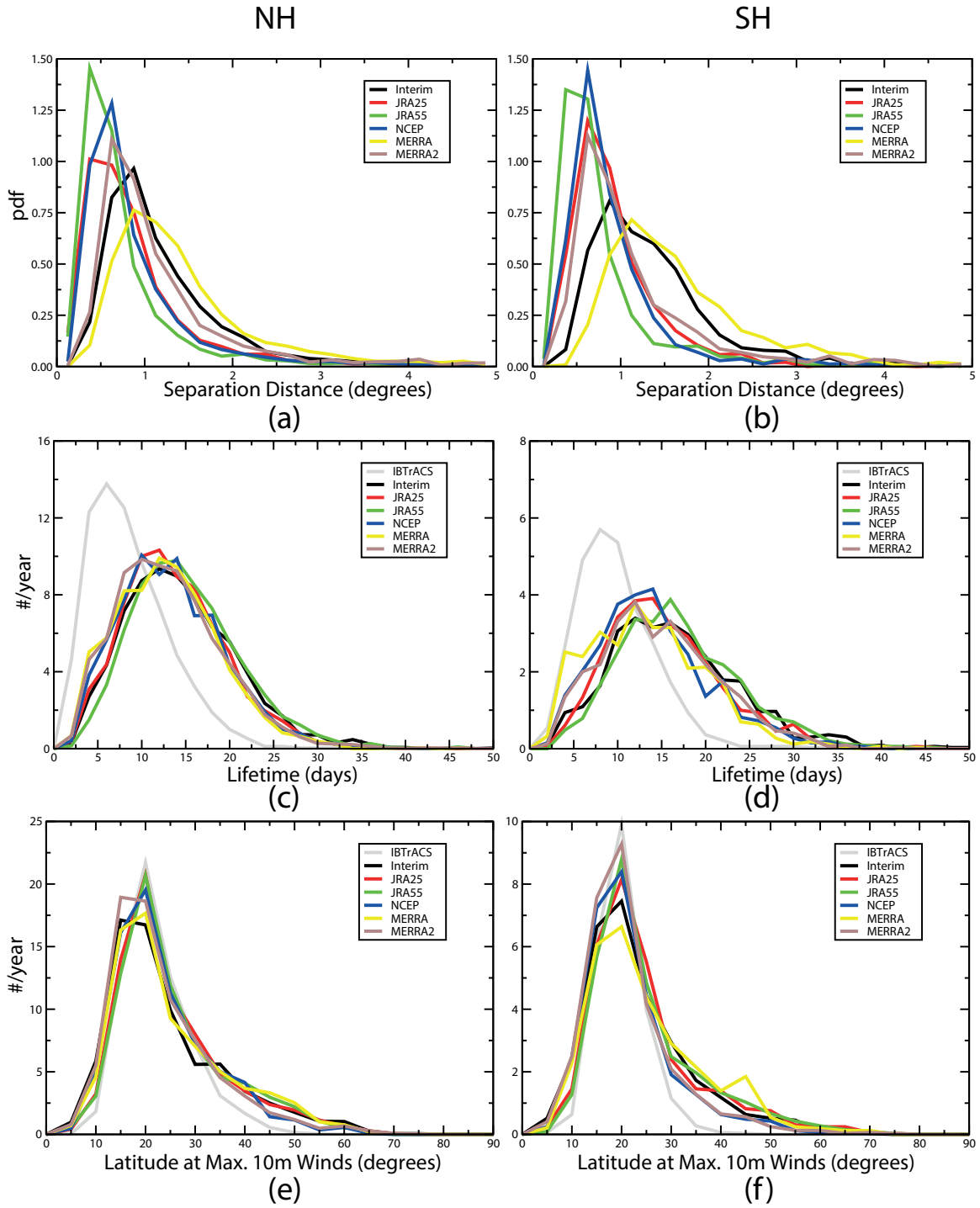
1023 **Fig. 2.** Distributions for the peak attained intensities of matched reanalysis and IBTrACS tracks  
1024 obtained using the direct matching method (c.f. Direct Matching Results subsection) based  
1025 on the MSLP, 10m winds and 925hPa winds (not for IBTrACS), (a) NH MSLP (hPa), (b)  
1026 SH MSLP (hPa), (c) NH 10m wind speed ( $m s^{-1}$ ), (d) SH 10m wind speed ( $m s^{-1}$ ), (e) NH  
1027 925hPa wind speed ( $m s^{-1}$ ), (f) SH 925hPa wind speed ( $m s^{-1}$ ). . . . . 54

1028 **Fig. 3.** Wind-pressure relationships for IBTrACS and each reanalysis and distributions for the radius  
1029 of maximum winds for the reanalyses based on the direct matching method (c.f. Direct  
1030 Matching Results subsection). (a) NH 10m wind speed versus MSLP, (b) SH 10m wind  
1031 speed versus MSLP, (c) NH radius of maximum winds and (d) SH radius of maximum winds. . . . . 55

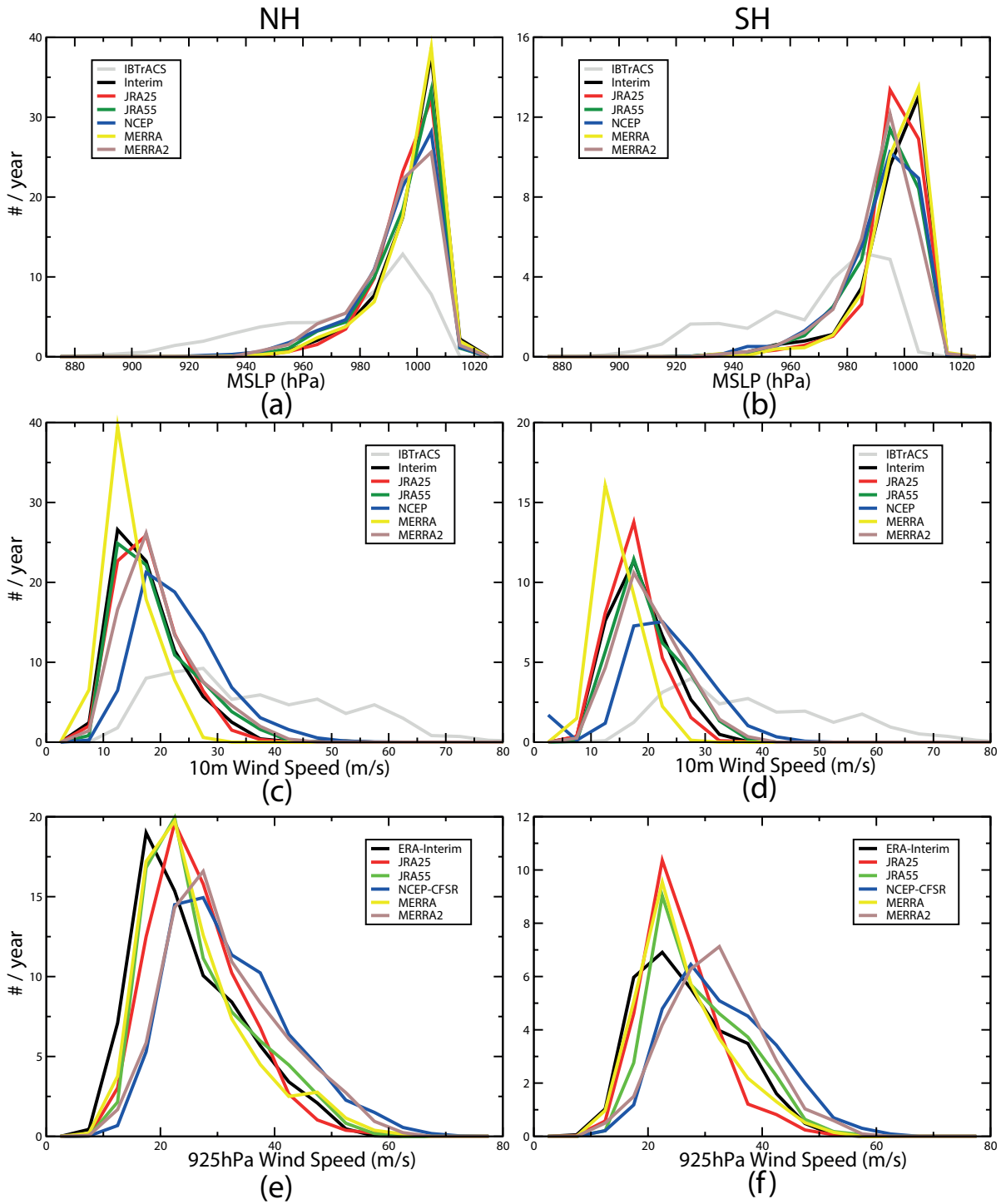
1032 **Fig. 4.** The seven basins used in this study, based on the IBTrACS definition. NI: North Indian,  
1033 WP: West Pacific, EP: East Pacific, NA: North Atlantic, SI: South Indian, SP: South Pacific,  
1034 SA: South Atlantic. . . . . 56

1035 **Fig. 5.** The average number of TCs per year for each of the seven basins for IBTrACS and identi-  
1036 fied in the reanalyses based on the objective detection method (c.f. Objective Identification  
1037 subsection). Vertical lines indicate the standard deviation. NI: North Indian, WP: West Pa-  
1038 cific, EP: East Pacific, NA: North Atlantic, SI: South Indian, SP: South Pacific, SA: South  
1039 Atlantic. . . . . 57

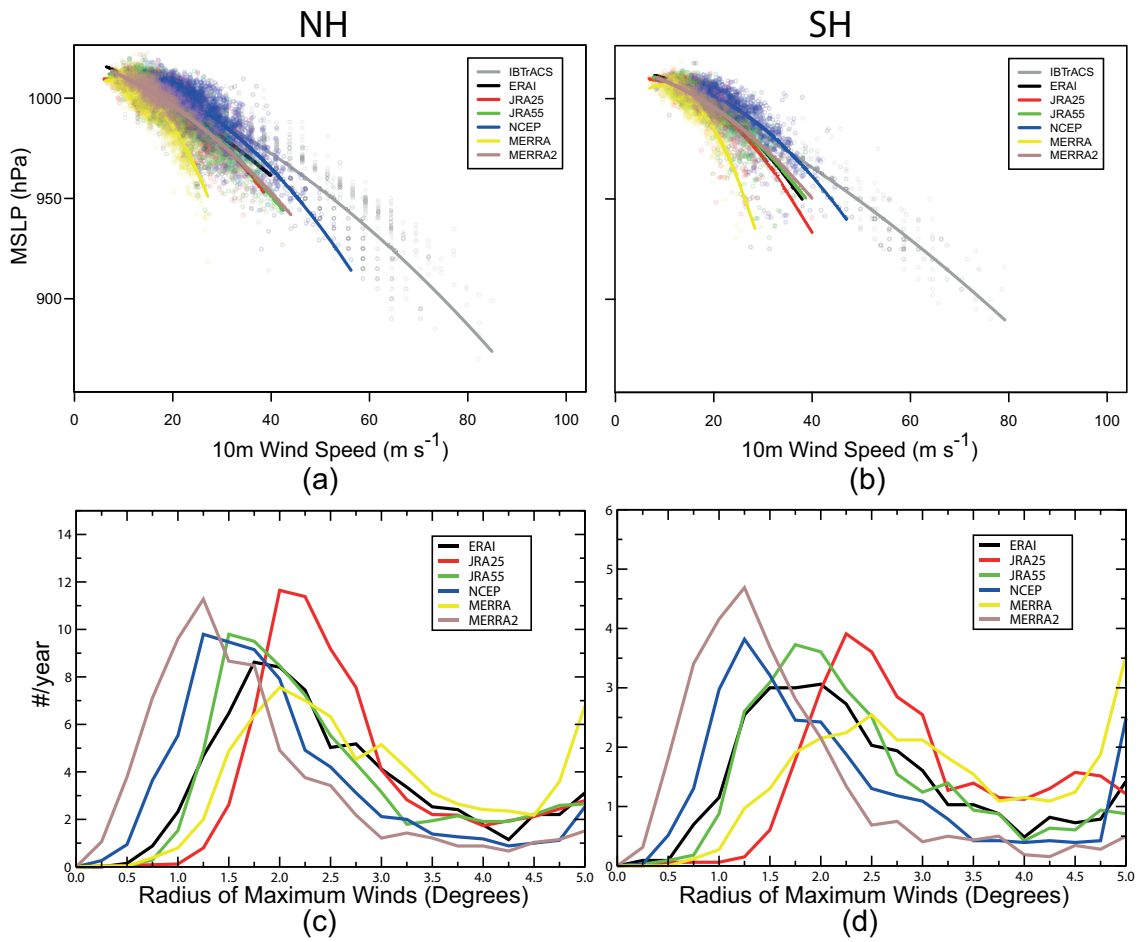
1040 **Fig. 6.** (a) Latitude at which genesis occurs in the SH for the objectively identified TCs in the  
1041 reanalyses that do not match with IBTrACS (number per year), (b) examples of two tracks  
1042 identified in the ERAI reanalysis with no matching track in IBTrACS, coloured dots indicate  
1043 10m wind speeds ( $m s^{-1}$ ), (c) MTSAT infrared satellite image of Storm 1 in (b) on 1800  
1044 UTC 1 Jan 2011 (d) GOES West infrared satellite image of Storm 2 in (b) on 1200 UTC 24  
1045 Dec 2011. . . . . 58



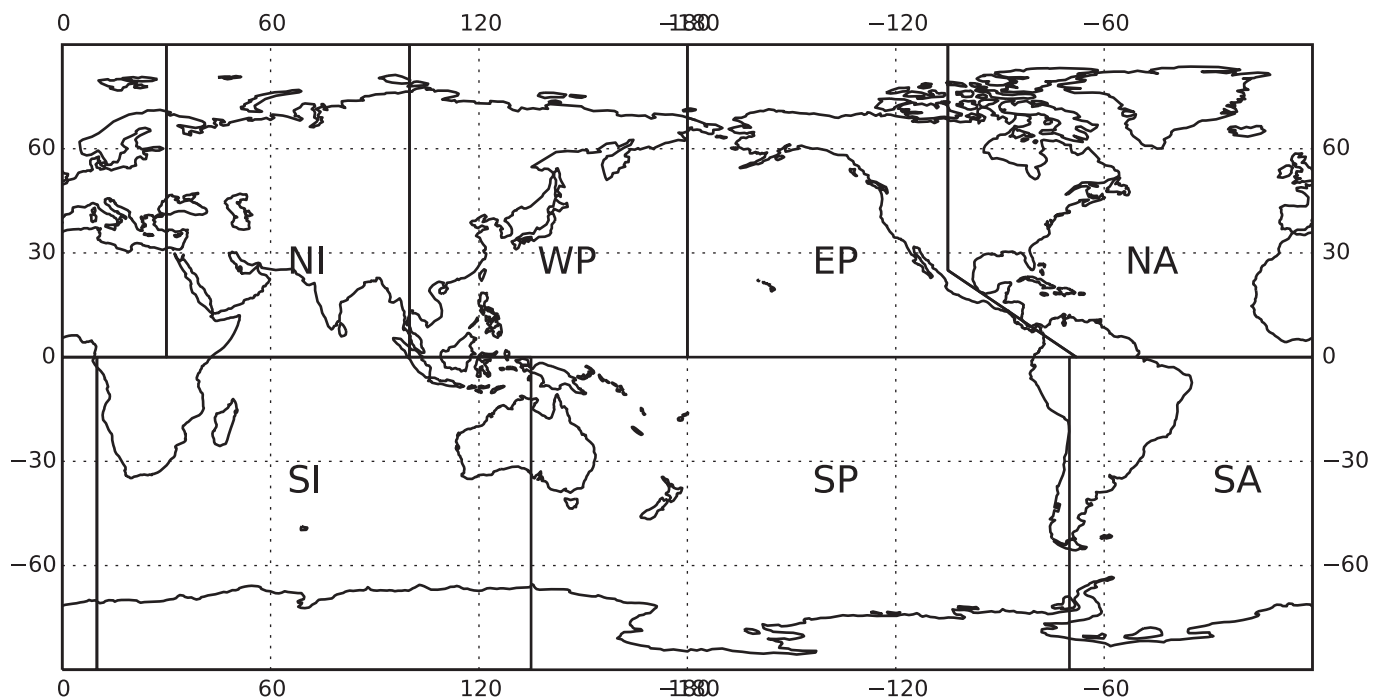
1046 FIG. 1. Distribution of mean separation distances (geodesic degrees,  $1^0 \simeq 111km$ ) between the reanalysis  
 1047 tracks and those of IBTrACS for tracks that match using the direct matching method (c.f. Direct Matching  
 1048 Results subsection) (a) NH, (b) SH, distribution of lifetimes (days) for the matched tracks (c) NH, (d) SH and  
 1049 the distribution of latitudes at which the matched tracks attain the peak intensity based on the 10m winds (e)  
 1050 NH, (f) SH.



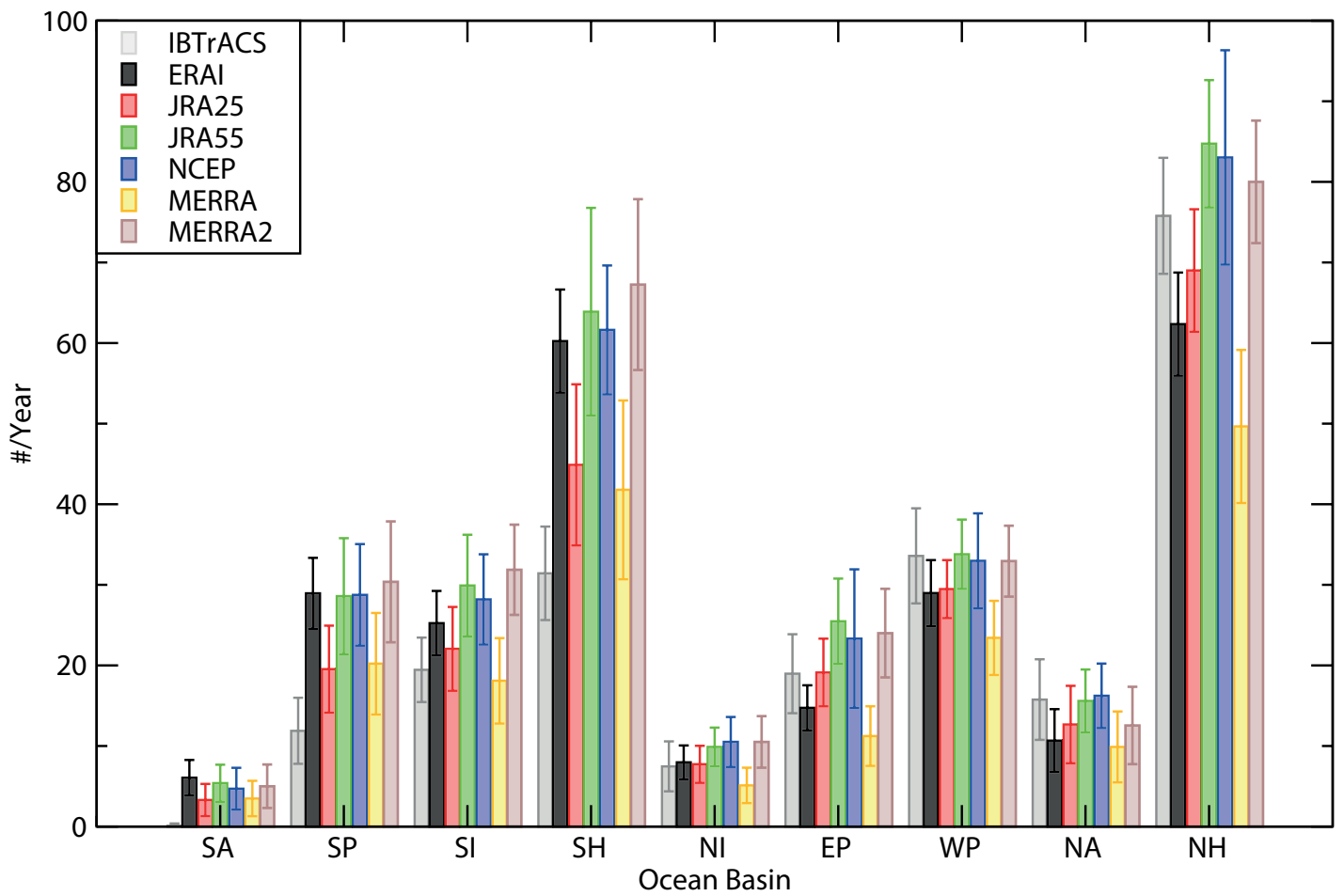
1051 FIG. 2. Distributions for the peak attained intensities of matched reanalysis and IBTrACS tracks obtained  
 1052 using the direct matching method (c.f. Direct Matching Results subsection) based on the MSLP, 10m winds and  
 1053 925hPa winds (not for IBTrACS), (a) NH MSLP (hPa), (b) SH MSLP (hPa), (c) NH 10m wind speed ( $\text{m s}^{-1}$ ),  
 1054 (d) SH 10m wind speed ( $\text{m s}^{-1}$ ), (e) NH 925hPa wind speed ( $\text{m s}^{-1}$ ), (f) SH 925hPa wind speed ( $\text{m s}^{-1}$ ).



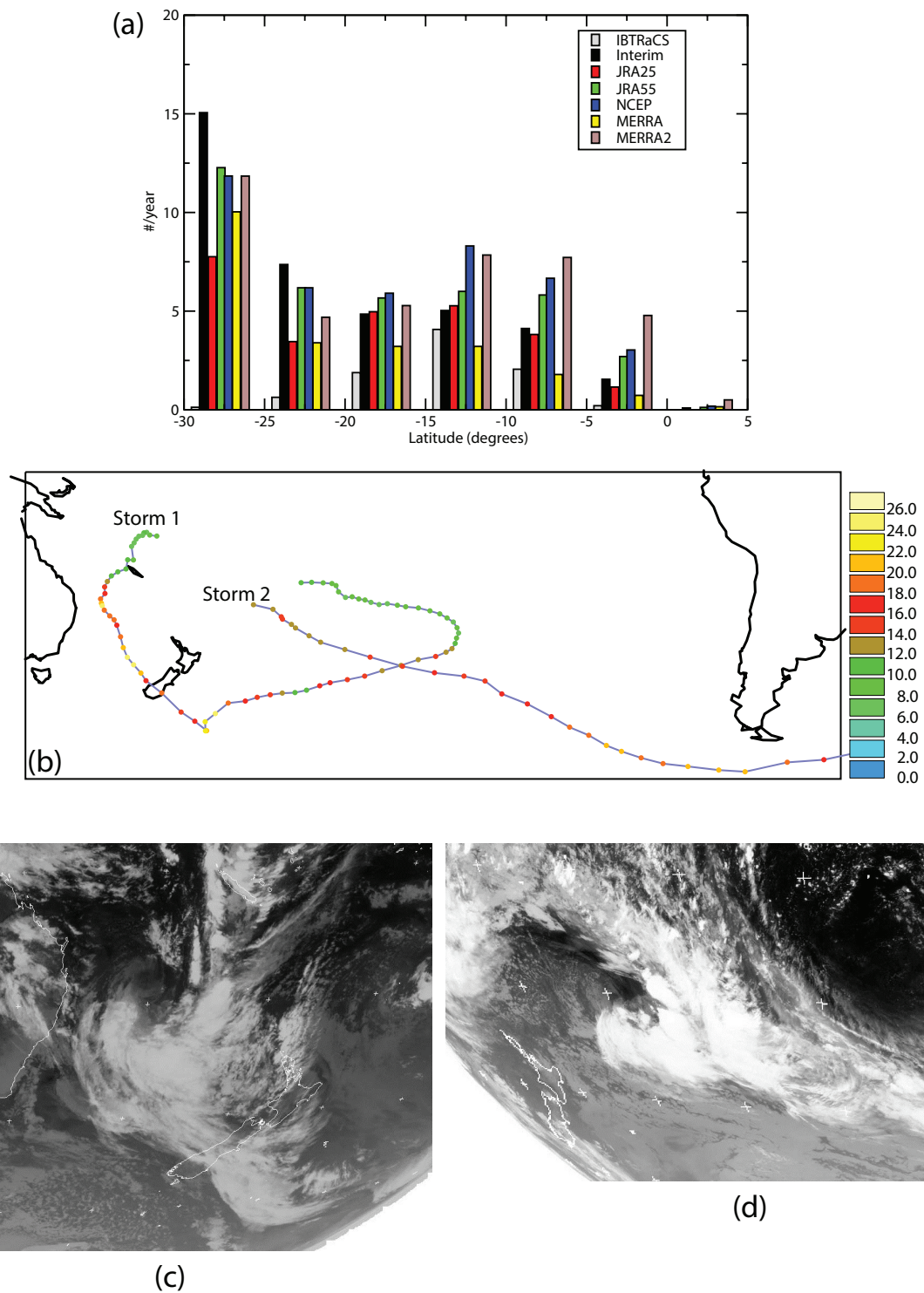
1055 FIG. 3. Wind-pressure relationships for IBTrACS and each reanalysis and distributions for the radius of max-  
 1056 imum winds for the reanalyses based on the direct matching method (c.f. Direct Matching Results subsection).  
 1057 (a) NH 10m wind speed versus MSLP, (b) SH 10m wind speed versus MSLP, (c) NH radius of maximum winds  
 1058 and (d) SH radius of maximum winds.



1059 FIG. 4. The seven basins used in this study, based on the IBTrACS definition. NI: North Indian, WP: West  
 1060 Pacific, EP: East Pacific, NA: North Atlantic, SI: South Indian, SP: South Pacific, SA: South Atlantic.



1061 FIG. 5. The average number of TCs per year for each of the seven basins for IBTrACS and identified in  
 1062 the reanalyses based on the objective detection method (c.f. Objective Identification subsection). Vertical lines  
 1063 indicate the standard deviation. NI: North Indian, WP: West Pacific, EP: East Pacific, NA: North Atlantic, SI:  
 1064 South Indian, SP: South Pacific, SA: South Atlantic.



1065 FIG. 6. (a) Latitude at which genesis occurs in the SH for the objectively identified TCs in the reanalyses that  
 1066 do not match with IBTrACS (number per year), (b) examples of two tracks identified in the ERAI reanalysis with  
 1067 no matching track in IBTrACS, coloured dots indicate 10m wind speeds ( $\text{m s}^{-1}$ ), (c) MTSAT infrared satellite  
 1068 image of Storm 1 in (b) on 1800 UTC 1 Jan 2011 (d) GOES West infrared satellite image of Storm 2 in (b) on  
 1069 1200 UTC 24 Dec 2011.